Composition and provenance of the Macigno Formation (Late OligoceneeEarly Miocene) in the Trasimeno Lake area (northern Apennines)

Ugo Amendola a, b, Francesco Perri b, Salvatore Critelli b, *, Paolo Monaco a,
Simonetta Cirilli a, Tiziana Trecci a, Roberto Rettori a
a Dipartimento di Fisica e Geologia, Universita` di Perugia, Piazza Universita`, 1, 06123 Perugia, Italy
b Dipartimento di Biologia, Ecologia e Scienze della Terra, Universita` della Calabria, via Ponte Bucci, 87036, Arcavacata di Rende (CS), Italy

ABSTRACT

Sandstone petrography and mudstone mineralogy and geochemistry of the Late OligoceneeEarly Miocene terrigenous deposits of the Macigno Fm. of the Trasimeno Lake area (Central Italy) provide new information on provenance, paleoenvironment, palaeoclimate, and geodynamics during the early stages of the northern Apennines foreland basin setting. Sandstones are rich in trace fossils and are quartz- ofeldspatic with various crystalline phaneritic (mostly granitoids) and medium-low grade metamorphic rock fragments. Volcanic and sedimentary lithic fragments are rare.

The mudstone mineralogy contains a large amount of phyllosilicates, quartz, and feldspars and small amount of calcite, which increases in the mid-part of succession.

Palaeoweathering indices (Chemical Index of Alteration with and without CaO value; CIA and CIA' respectively) suggest a source area that experienced low to moderate weathering and low recycling processes (on average, CIA ¼ 66.4 and CIA' ¼ 69.7). Furthermore, very low and homogeneous values of

Rb/K ratios (<0.006) suggest weak to moderate weathering conditions.

The sandstone and mudstone composition reflects a provenance derived from uplifted crystalline rocks. The different amount in feldspars, the variety of lithic fragments, the occurrence of mafic and carbonate input, coupled with evidence of multi-directional flows, suggest a provenance from

different source areas. The geochemical proxies indicate a provenance from both felsic and mafic sources, pre- dominantly for the Maesta` section that shows Cr/V values ranging from 1.15 to 3.36 typical of source areas composed of both felsic and mafic rocks. The Western-Central Alps are inferred to be the main source area of the Macigno foreland system, but significant signals from the Mesomediterranean Microplate are also testified. These new data suggest that the Macigno Fm. was probably located in a peculiar area which received either distal fine turbidite flows from the northernmost Alpine area and residual sandy debris flows coming from the westernmost Alps

Keywords: *Composition, Provenance, Gravity flow deposits Northern Apennines, Palaeoweathering, Palaeoenvironment*

1. INTRODUCTION

The thrust belt-foreland system of Northern Apennines was characterized by a continuous eastward migration of depocentres reflecting detachment of subducted lithosphere as result of African-European collision in the Late

1998; Dinelli et al., 1999; Barsella et al., 2009). During the Oligo- ceneeMiocene, foredeep depocentres were filled by thick debris of turbidite deposits in continuous and complex depositional units. The Macigno Fm. represents the first depositional unit of the Late OligoceneeEarly Miocene foreland basin system of northern Apennines, linked to Alpine sectors through longitudinal feeding of the foreland basin (Ricci Lucchi, 1986, 1990). The Macigno Fm. is traditionally divided into a westernmost and oldest portion (late Chattian), cropping out along the Tuscan coast and named “Macigno Costiero” and an eastern and younger portion (late Chattian-Aquitanian) named “Macigno Appenninico” thrust eastward on the Marnoso-arenacea Formation in the Casentino area (Boccaletti et al., 1990; Milighetti et al., 2009 among others). The ModinoeCervarolaeTrasimeno units and associated facies (now included in eastern Macigno) and the overlying Marnoso-Arenacea Fm. represent the Mid-Late Miocene foreland basin sys- tem, whereas, the depositional framework and basin architecture of the foreland system are well developed (Ricci Lucchi, 1986,

1990; Centamore et al., 2002; Guerrera et al., 2012b). Differently to Ricci Lucchi (1986, 1990), Valloni et al. (1991), Pandeli et al. (1994) and recently Barsella et al. (2009) indicated only one terrigenous source area for the Macigno Fm., identified with the western-central Alps. Other authors recently claim that alpine source interfingered with an increasing contribution from the emerging Apennines from the Early Miocene onward, involving the upper portion of the Macigno Formation, especially the ModinoeCervarola unit (Gandolfi et al., 1983; Andreozzi and Di Giulio, 1994; Di Giulio, 1999). According to Cornamusini (2002) and Cornamusini et al. (2002), new sedimentological and petrographic data suggest that the Corsica- Sardinian Hercynian basement is the source area of the debris flow and turbidite sandstones of the "Macigno Costiero". Thus, the hypothesis indicating a multi-source area for the Macigno Fm. can be strongly considered. In other models, a provenance from the Mesomediterranean microplate can also be suggested (e.g. Guerrera et al., 2012a, 2012b; Perrone et al., 2013; Guerrera and Manuel Martín-Martín, 2014, and bibliography therein).

Changes in sandstone composition of perisutural basins usually reflect complex provenance relationships from local to distal source areas, where long-distance transport is generally associated with Apenninic longitudinal orientation of flows. The local derivation of terrigenous, coarse grained and massive material is generally transverse from the west (e.g. Zuffa, 1987; Critelli et al., 1990; Critelli, 1993). This mixed provenance is typical of remnant ocean basin-fill (Critelli et al., 1990; Critelli, 1993) and foreland basin systems (Zuffa, 1987; Critelli, 1999; Critelli et al., 2007).

The aim of this work is to use a multi-disciplinary approach to provide useful information on the provenance of the Macigno Fm. sandstones for unraveling both local and distal terrigenous dispersal. For this purpose a detailed study of the Late Oligocene- eEarly Miocene sandstones and mudstones characterizing the Macigno Fm. of the Trasimeno Lake area, previously analyzed by sedimentological and ichnological point of view (Monaco and Trecci, 2014), has been done. The petrographical, mineralogical, and geochemical proxies are aimed to better understand the composition, provenance, and paleoclimatic signatures during the development of a foredeep basin

system. Petrographic study of the coarse-grained fraction coupled with chemical and mineralogical analyses of the fine-grained fraction represents a thorough tool to investigate the processes that occurred from sediment generation on the exhumed uplands to the final deposition on foredeep basins. Detrital modes of sand reflect the cumulative effects of source rock composition, chemical weathering, hydraulic sorting, and abrasion (Suttner, 1974; Basu, 1985; Johnsson, 1993; Nesbitt et al., 1996). The distribution of major and trace elements related to the mineralogical composition of fine-grained sediments is an impor- tant factor to reconstruct the source-area composition, the weathering and the diagenetic processes (e.g. Condie et al., 1992, 2001; Bauluz et al., 2000; Mongelli et al., 2006; Critelli et al., 2008; Zaghloul et al., 2010; Caracciolo et al., 2011; Perri, 2014; Perri and Ohta, 2014).

The X-ray diffraction (XRD) and X-ray fluorescence spectrom- etry (XRF) have been used to study and characterize the mineral- ogical and chemical variations of the mudstone samples, whereas the sand fraction has been studied by petrographic analysis. By combining the information deduced from these analyses, it is possible to outline possible variations on source areas and, thus, to explain and predict the sedimentary evolution and geological processes affecting the studied sediments. Moreover the relationship developed between source area and sedimentary basin can be also defined.

2. GEOLOGICAL SETTING

The Northern Apennines are basically composed of two tectonic complexes: (1) the remnants of a CretaceousePaleogene accre- tionary wedge (Ligurian Complex), generated by the AfricaeEurope convergence, thrust on top by (2) an OligoceneeMiocene terrige- nous complex (Ricci Lucchi, 1986) that was accreted in a retreating subduction zone overriding the Adriatic continental margin (e.g., Castellarin, 1992). This second terrigenous complex is composed of different units: the Macigno and Modino turbiditic units of late Chattian to early Aquitanian age (25e23 Ma), the Monte Cervarola Fm. of late Aquitanian to early Langhian age (21e16 Ma), and the Marnoso-arenacea Fm. of Langhian to Tortonian age (14e9 Ma) (Guerrera et al., 2012b) (Fig. 1). The Late

Oligocene - Early Miocene Macigno foredeep system was a basin 250e300 km in length, almost 50 km in width, and NWeSE oriented, starting from the modern Emilia (Northern Italy) to the Latium-Umbria border (Hill and Hayward, 1988; Boccaletti et al., 1990). The studied sections outcropping at the north of Trasimeno Lake (Fig. 2) belong to a NeS elongated Macigno Fm. basin deposited in the Tuscan Domain that were overthrust eastwards over the innermost sedimentary suc- cessions of the Umbria Domain (Canuti et al., 1965).

In the northern area of the Trasimeno Lake, the Macigno Fm. overlies the Scaglia Toscana Fm. (Cretaceous e Late Eocene) (Piccioni and Monaco, 1999; Plesi et al., 2002). The Scaglia Toscana Fm. (about 200 m thick) is made of limestones, marly limestones, variegated marls and dark pelitic beds with many coarse-to very fine-grained grained turbidites (Damiani et al., 1987; Ielpi and Cornamusini, 2013; Monaco et al., 2012). The Middle-Late Eocene portion is characterized by mud turbidites containing a typical deep-sea Nereites ichnofacies, with an ichnocoenosis at Ave- toichnus luisae, Chondrites intricatus, Cephalotes targionii, Cla- dichnus, Taenidium and Ophiomorpha rudis (Monaco et al., 2012). These deposits show an increasing upwards contribution of clayey- marly and clayey lithotypes, respectively (Piccioni and Monaco, 1999; Monaco and Uchman, 1999; Monaco et al., 2012).

The Macigno Fm. is subdivided into three members: the Molin Nuovo Member (MAC1), the Poggio Belvedere Member (MAC2), studied in detail in this work, and the Lippiano Member (MAC3) (see detailed description in Trecci and Monaco, 2011). The Molin Nuovo Member in the lower portions of the Macigno Fm. (500e600 m of maximum thickness), consists of thick-bedded turbidites that pass upward to thinner strata. Facies assemblages indicate various deposits (in lithology and thickness), often ar- ranged in thickening-upward sequences that can be related to depositional lobes of deep-sea fan (sensu Einsele, 1991). Thickening upward sequences are present even in the basal part of the Poggio Belvedere Member, while stationary sequences are common in the middle-upper portion of the Lippiano Member. Thick-bedded sandstones of outer lobes are interbedded with thinner arenaceous-pelitic and calcareous turbidites and lobe-fringe de- posits of

basin plain. The maximum thickness of the Poggio Belvedere Member is about 300 m, and its age has been attributed to the Chattian (MNP25b subzone, see Plesi et al., 2002 for the micropaleontological content). The lower units contain slurried beds (Ricci Lucchi and Valmori, 1980) and carbonate turbidites (Bruni and Pandeli, 1980; the Pietralavata Key-bed of Plesi et al., 2002; Brozzetti, 2007). Similar carbonate turbidites (the Polvano Bed) are described by Aruta et al. (1998) for the Cortona area (Brozzetti, 2007). Nannofossil assemblages (Plesi et al., 2002) testify the Late Chattian-Early Aquitanian age (MNP25b-MNN1b) for the Poggio Belvedere Member. In the overlying Lippiano Member, the thinner facies, tabular beds (with flat basal surfaces and good lateral continuity, sensu Einsele, 1991) are dominant, typically of distal, basin plain environment. The calcareous beds are more frequent than in the Poggio Belvedere Member (Aruta, 1994; Aruta and Pandeli, 1995; Aruta et al., 1998). Biostratigraphic investigation (Plesi et al., 2002) suggests a Late Aquitanian age (MNP25b-MNN1b) for the Lippiano Member. In the overall Macigno Fm., multidirectional grooves and flute casts indicate mainly NW/SE oriented paleocurrents, with a SE preferential flow direction, and minor W oriented flows (e.g. slurried beds and slumps) (see in detail below).

3. Stratigraphy, facies and ichnocoenoses of the studied sections

Three stratigraphic sections belonging to Poggio Belvedere Mb. (MAC2) have been studied in the Trasimeno Lake area (Fig. 2), and were sampled for the purposes of the present study. The studied sections were sampled near Cortona along the SP35 road from Cortona (Tuscany) to Umbertide (Umbria) in three distinctive areas where are in stratigraphical continuity: the Pianello, Renali and Maestà Stratigraphic sections (Fig. 3).

3.1. Pianello Stratigraphic section

The section (Fig. 4AeC) is more than 25 m in thickness and rests on the Early Oligocene Molin Nuovo Mb. (MAC1). The Pianello section is characterized by a diverse facies assemblage that

157 includes massive to laminated thin-bedded coarse-grained turbidite sand- stones (F5eF6eF7 facies
158 of Mutti, 1992), up to 2e4 m in thickness, 0.5 m thick slurried beds (F1eF2 facies of Mutti, 1992)
159 and an alternance of bioturbated hemipelagic mudstones and fine-grained turbidites (F8eF9aeb
160 facies of Mutti, 1992).
161 The sandy horizons have been interpreted as transitional high- density turbidites (Mutti, 1992) or
162 cohesive sandy debris flow de- posits (Shanmugan, 2002). They partially include pebbles, mud
163 lumps and several vegetal fragments and decrease in thickness going toward the mid-upper portion
164 of the section in which the mudstones and mud turbidites begin to prevail. Fine-grained turbidites
165 contain plane-parallel and convolute laminae and are associated to the Tbee Bouma facies. These
166 levels include a rich ichnocoenosis, typical of basin plain depositional area of the *Nereites*
167 ichnofacies, mainly represented by hypichnial to epichnial and exichnial trace fossils (Monaco and
168 Trecci, 2014). The abundant trace fossils are *Halopoa imbricate, Phycosiphon sp., Spirophycus*
169 *bicornis*. The common trace fossils are *C. intricatus, Ophiomorpha rudis, Ophiomorpha annulata,*
170 *Trichichnus* sp., *Spirorhaphe involuta*, whereas *Palaeophycus tubularis* is rare.
171 Slurried beds are easily recognizable for the inner subdivision of the beds in three intervals: a)
172 coarse-grained basal sandstone interval, b) an intermediate swirly appearance (sensu Ricci Lucchi
173 and Valmori, 1980) and, on the top, c) a fine-grained sandstone interval referred as F9a (Trecci and
174 Monaco, 2011 and references therein). Slurried beds occur through the entire stratigraphical section
175 and they are often intercalated with fine-grained turbidites. They come from a close slope area and
176 probably are derived from co-genetic debrite-turbidite composite flows (Ricci Lucchi and Valmori,
177 1980; Talling et al., 2004; see types of Muzzi Magalhaes and Tinterri, 2010).
178 Palaeocurrent data show predominant NW-oriented flows for fine-grained turbidites and some
179 massive sandy horizons. However several groove casts, individuated in the uppermost facies of the
180 coarse-grained sandstones and slurried divisions, clearly indicate W-oriented flows (Fig. 4B). Thus
181 two types of groove casts have been recovered with an angle from 20 to 40◦. The facies assemblage

of Pianello Stratigraphic section reflects a transition from outer lobe, indicated by coarse-grained sandstone horizons, to fringe- basin plain facies, represented by fine-grained turbidites, and outlines a slight deepening of the depositional system.

3.2. Renali Stratigraphic section

The section (Fig. 4D) is more than 20 m thick and overlies de- posits of the Pianello section. The section is characterized by an increase of rhythmical fine-grained turbidites (F9aeb facies). Laminated beds (Tb of Bouma facies) are thicker than the convolute laminae interval (Tc of Bouma facies) and they can reach 1 m in thickness.

Ichnocoenosis is quite similar to that analyzed in the previous section. Differences consist of larger amounts of *Ophiomorpha annulata, Halopoa, Phycosiphon, Planolites* and *Spirorhaphe*. Similarly to previous section *Spirophycus bicornis* is abundant whereas *Paleodictyon maximum* and *P. strozzii* are common. Also *Helmintorhaphe* sp. and *Cosmorhaphe lobata* occur (Fig. 5AeB) (Monaco and Trecci, 2014). Coarse-grained sandstone facies (F5eF6eF7 facies), up to 2 m thick, only appear in the basal and upper portion, and they are totally absent in the central part where fine-grained tur- bidites are dominant. Slurried beds, up to 1.5 m thick, show similar characteristics to those described for the previous section but they are less frequent. Moreover, in the basal portion of analyzed sec- tion, laminated to convoluted calciturbidite deposits, up 2e3 m thick, occur (Fig. 4D). They are well sorted, and have sharp basal contacts and tabular top surfaces and that include graded and laminated to convoluted Bouma Taee facies (Trincardi et al., 2005; Monaco et al., 2009; Trecci and Monaco, 2011).

Paleocurrent data show a NW-oriented flow for fine-grained turbidite facies. As seen in the previous section, multi-directional flows have been observed. In some thin laminated beds (F9b facies) flute casts clearly indicate W-oriented turbidite flows although groove casts individuated in calciturbidite levels show paleoflows towards the S and SW. The facies assemblage of Renali area

thus reflects a basin plain environment, which locally received gravity flows coming from a very close slope area.

3.3. Maesta` Stratigraphic section

The section (Fig. 4EeF) is more than 20 m thick and overlies deposits of Renali section and is overlain by Early Miocene Lippiano Mb. (MAC3). The section consists of mostly rhythmical, fine-grained turbidites (F9a-b facies) up to 5e6 m thick, which are interfingered by thin slurried beds, up 0.5 m thick and thin-bedded coarse-grained sandstones (F4eF7eF8 facies of Mutti, 1992), up 0.5e0.7 m thick. Laminated and convoluted facies (F9a-b facies of the same Author, Fig. 4F) are thinner than the Renali section, and the mudstone intervals are more abundant. The ichnocoenosis is dominated by an abundant endichnial/hypichnial Halopoa (both *Hydrostachys embricata* and *H.* var. f*ucusopsis*), which occur in conspicuous amount in every thin beds, with Spirorhaphe involuta and *Urohelminthoida dertonensis*. *Chondrites, Paleophycus, Planolites, Ophiomorpha* and *Trichichnus* are rarer than in previous sections. Of particular significance is the occurrence of large *Spirophycus bicornis* with abundant *Spirorhaphe involuta, Paleodictyon minimum*. Also *P. strozzii* and *Urohelminthoida dertonensis* occur (Fig. 5CeF) (Monaco and Trecci, 2014).

Paleocurrent data only show NW-oriented flows. The Maesta` section facies indicate a deeper basin plain environment, locally with turbidites and other residual gravity flows coming from a slope area that was probably farer than the depositional system depicted for Renali area.

4. Sampling and analytical methods

Sandstones and mudstones were sampled along the Poggio Belvedere Mb. (MAC2) in the Cortona area (Figs. 2 and 3). The sampling was concentrated in those parts of the succession, which are better exposed and preserved and thicker than in other analogue area of Trasimeno Lake. For the purpose of this study, we selected and analyzed only sandstone strata. Some strata show abundant carbonate particles (Renali area) characterized by car- bonate clasts and fossils in both graded and

laminated turbidite facies. These samples were only qualitatively described and not included in the recalculated analysis of the sandstones.

Nineteen medium-to coarse-grained sandstone samples were selected for thin-section preparation and modal analysis. Thin sections were etched with HF and stained by immersion in sodium cobaltonitrite solution to allow the identification of feldspars. More than 400 points were counted through the use of a petrographic microscope in each thin section according to the Gazzi-Dickinson method (Gazzi, 1966; Dickinson, 1970; Ingersoll et al., 1984; Zuffa, 1985). Recalculated grain parameters are defined according to Dickinson (1970), Ingersoll and Suczek (1979), Zuffa (1985), Critelli and Le Pera (1994, 1995), and Critelli and Ingersoll (1995).

Mudstone samples were crushed and milled in an agate mill to a very fine powder. The powder was placed in an ultrasonic bath at low power for a few minutes for disaggregation.

The mineralogy of the whole-rock powder was obtained by X- ray diffraction (XRD) using a Bruker D8 Advance diffractometer (CuKa radiation, graphite secondary monochromator, sample spinner; step size 0.02; speed 1 s for step) at the University of Calabria (Italy). Semiquantitative mineralogical analysis of the bulk rock was carried out on random powders measuring peak areas using the WINFIT computer program (Krumm, 1996). The strongest reflection of each mineral was considered, except for quartz for which the line at 4.26 Å was used instead of the peak at 3.34 Å because of its superimposition with 10 Å-minerals and IeS mixed layer series. The abundance of phyllosilicates was estimated measuring the 4.5 Å peak area. The percentage of phyllosilicates in the bulk rock was split on the diffraction profile of the random powder, according to the following peak areas: 10e15 Å (illi- teesmectite mixed layers), 10 Å (illite micas), and 7 Å (kaolini- te chlorite) minerals (e.g. Cavalcante et al., 2007; Perri, 2008).

Whole-rock samples were prepared by milling to a fine powder in an agate mill. Elemental analyses for major and some trace ele- ments (Nb, Zr, Y, Sr, Rb, Ba, Ni, Co, Cr, and V) were obtained by X-ray fluorescence spectrometry (XRF) using a Bruker S8 Tiger equipment at the University of Calabria (Italy), on pressed powder disks of whole-rock samples. These data were compared to

international standard-rock analyses of the United States Geological Survey (e.g., Flanagan, 1976). The estimated precision and accuracy for trace element determinations are better than 5%, except for those ele- ments having a concentration of 10 ppm or less (10e15%). Total loss on ignition (L.O.I.) was determined after heating the samples for 3 h at 900 ◦C.

5. Sandstone petrology and detrital modes

Samples include massive coarse-grained sandstones from the lobe-fringe facies (from F5 to F7 facies; Mutti, 1992), slurried divisions (F2 facies; related to residual dense flows), related to residual dense flows, and graded-laminated sandstones from rhythmical fine turbidites (F8eF9a-b facies; related to low-density flows), related to low-density flows. The studied quartzofeldspathic sandstones are composed of moderately to poorly sorted, silici- clastic grains.

Raw point-count data of sandstones are in Table 1, whereas the recalculated modal point-count data are in Table 2.

a) Pianello Stratigraphic Section

Sandstones of the Pianello area range from massive sandstones of an outer lobe facies (P1, P23, P3, P5 samples) to fringe deposits of a basin plain (P2, P21, P22, P18 samples) with a single sample from a slurried division (P26 sample). The quartzofeldspathic sandstones have an average composition of $Qm_{48}F_{40}Lt_{12}$ (Fig. 6), and the Qm/F (Quartz monocrystalline/Feldspars) ratio is 1.33. These sandstones have variable sedimentary versus metasedimentary lithic frag- ments (average value: $Lm_{86}Lv_{1}Ls_{13}$; outer lobe facies: $Lm_{83}Lv_{3}Ls_{34}$; fringe-basin plain: $Lm_{88}Lv_{0}Ls_{12}$; slurried division: $Lm_{89}Lv_{0}Ls_{11}$; Fig. 6; Table 2). Feldspars (both plagioclase and K-feldspars) are the most abundant

285 constituents in the lobe-fringe facies ($Qm_{39}F_{46}Lt_{15}$; Qm/F ¼ 0.94). In particular
286 feldspar content reaches the highest content in W-oriented grain flow deposits of the
287 lobe facies (i.e. P5 $Qm_{36}F_{49}Lt_{15}$; Qm/F 0.73) of the mid-upper portions of the
288 stratigraphic section. Plagioclase is dominant (average P/F 0.66), and fresh grains are
289 slightly more abundant than altered ones. Some plagioclase crystals display albite
290 polysynthetic twinning (Fig. 7A). Quartz grains are also abundant, mainly as mono-
291 crystalline subrounded to angular and subspherical grains. Quartz grains are more
292 prevalent in fringe-basin plain facies ($Qm_{55}F_{34}Lt_{11}$; Qm/F 1.65) and slurried divisions
293 ($Qm_{56}F_{39}Lt_5$;Qm/F 1.44) than in the external lobe sandstones. Polycrystalline grains
294 also occur in large amounts ($Qp_{73}Lvm_1Lsm_{26}$) and have similar tectonics-fabric versus
295 plutonic-fabric. Dense minerals include garnet, epidote and zircon. Metasedimentary
296 lithic grains are not abundant and they include phyllite, slate and fine-grained
297 micaschist (Fig. 7B). Sedimentary rock fragments occur in discrete amounts in the outer
298 lobe facies (i.e. P23 sample). A few volcanic lithic grains are also present (P23 sample)
299 and they exhibit a felsic granular texture with plagioclase and minor quartz phenocrysts
300 (Fig. 7C). Abundant phaneritic fragments of plutonic rocks, mostly plagioclase-rich
301 granodiorite and tonalite, with minor granite (Fig. 7D), and coarse gneissic fragments
302 also occur (average value; $Rg_{70}Rs_3Rm_{27}$; outer lobe facies: $Rg_{66}Rs_5Rm_{29}$; distal
303 turbidite facies: $Rg_{73}Rs_2Rm_{25}$; slurried division: $Rg_{73}Rs_3Rm_{24}$). In the outer lobe facies
304 samples, several high-medium grade metamorphic (Fig. 7E) and some sedimentary
305 fragments occur.

306 Lithic fragments, especially felsic volcanic fragments, in sand- stone modes of the
307 Pianello area are less abundant than those from the Macigno Fm. (Fig. 8; Table 3). In
308 detail, sandstones of outer lobe facies are more feldspar-rich than sandstones of both
309 “Macigno Appenninico” of Northern Tuscany (Di Giulio, 1999: $Qm_{59}F_{29}Lt_{17}$; Bruni et
310 al., 2007: average value, $Qm_{50}F_{34}Lt_{16}$) and the “Macigno Costiero” of Southern
311 Tuscany (Cornamusini, 2002: $Qm_{57}F_{19}Lt_{24}$). Also Poggio Belvedere sandstones of this

¼

312 study are more feldspar- rich than sandstones analyzed by Barsella et al., 2009 ($Qm_{36-61}F_{14-24}Lt_{10-25}$; Fig. 8). However, Plesi et al (2002) report a similar feldspar-rich trend in
313
314 the lower sandstones of Poggio Belvedere Mb. collected in the High Tiber valley
315 (Umbria). Likely, Bruni et al. (2007) point out a slight feldspar enrichment at the
316 transition of the Lower-Upper Macigno Fm. in Abetone area (NW Tuscany) (max F
317 35.6%, $Qm_{44}F_{44}Lt_{12}$; see GO 24 sample in Fig. 8). Differently, sandstones of basin plain
318 facies have a composition that can be comparable with the average value indicated for
319 the Macigno Fm. (Valloni et al., 1991; Di Giulio, 1999; Bruni et al., 2007; Barsella et al.,
320 2009) (Table 3).

321 b) Renali Stratigraphic Section

322

323 Sandstones collected along the Renali stratigraphic section are in outer lobe-fringe
324 facies (R7 and R3 samples), basin plain facies (R12 and R5 samples) and slurried
325 divisions (R10 and R15 samples). Other samples were collected in the calcareous
326 turbidite facies (R1, R2 and R9 samples) but they were not counted but only qualita-
327 tively described. The sandstone composition is quartzofeldspathic (average value:
328 $Qm_{59}F_{30}Lt_{12}$; outer lobe-fringe facies: $Qm_{61}F_{30}Lt_{9}$; basin plain facies: $Qm_{56}F_{32}Lt_{12}$;
329 slurried division: $Qm_{60}F_{27}Lt_{13}$). The average Qm/F ratio is 1.93.

330 These sandstones have similar amounts of sedimentary versus metasedimentary lithic
331 fragments (average value: $Lm_{63}Lv_{11}Ls_{26}$; outer lobe facies: $Lm_{69}Lv_{19}Ls_{12}$; basin plain
332 facies: $Lm_{61}Lv_{13}Ls_{26}$; slurried division: $Lm_{57}Lv_{1}Ls_{42}$; Fig. 6). Quartz grains are the
333 most abundant constituents in all the sampled facies and their amount remain almost
334 homogeneous with a slight peak in the outer lobe facies. Quartz grains show the same
335 textural characteristics seen in the previous section, with a sharp prevalence of
336 monocrystalline grains on polycrystalline grains, more marked than in the previous
337 section ($Qp_{54}Lvm_{9}Lsm_{37}$) (Fig. 7F). Feldspars (both plagioclase and K-feldspars) are

also abundant and maintain a constant ratio with the quartz grains. Many feldspar grains are altered; they aresericitized and partially clay altered. The plagioclase versus total feldspars ratio is higher than that of the previous section (P/ F 0.74). Metasedimentary lithic grains are not so abundant and they include phyllite, slate and fine-grained micaschist, including also few chloriteschist fragments. Siltstone and chert fragments are also present. Volcanic lithic fragments are more abundant than in the other sections (with a prevalence in R7 sample) and they occur in both outer lobe and distal turbidites facies (Fig. 7G). Abundant phaneritic fragments of plutonic rocks, mostly plagioclase-rich granodiorite and tonalite, with minor granite also occur (average value $Rg_{65}Rv_{3}Rm_{32}$; $Rg_{62}Rs_{9}Rm_{29}$). Coarse gneissic fragments are rare. Micas grains, including either muscovite, biotite and chlorite, are abundant. Carbonate constituents are only present in R1, R2, and R9 samples, collected within calciturbidite levels, and R10 sample (Fig. 7H). Biofacies related to these levels are reported in detail in 5.1.

The interstitial component of siliciclastic arenites includes detrital fine siliciclastic matrix, and rare authigenic minerals and pseudomatrix. Only in the carbonate samples the interparticle porosity is partially filled by sparite and microsparite calcite cement and relatively fine carbonate matrix. Differently to previous data of the Macigno Fm., the Renali sandstones are quite similar to those of the "Macigno Appenninico" of Northern Tuscany (Di Giulio, 1999: $Qm_{59}F_{29}Lt_{17}$; Bruni et al., 2007: average value, $Qm_{50}F_{34}Lt_{16}$) and the Poggio Belvedere Mb. sandstones of Trasimeno Lake area (Plesi et al., 2002; $Qm_{40\text{-}55}F_{20\text{-}50}Lt_{10\text{-}25}$; Barsella et al., 2009; $Qm_{36\text{-}61}F_{14\text{-}24}Lt_{10\text{-}25}$; Table 3). The lithic composition is quite similar to that reported by Cornamusini (2002) for the Macigno Costiero in Southern Tuscany ($Lm_{66}Lv_{19}Ls_{15}$). The volcanic lithic percentage is similar (Renali area: Lv 13; Macigno Costiero: Lv > 13) although the means of volcanic index (Iv Lv/L%) is properly more compatible with Macigno Fm. of Chianti Hills area (Renali: Iv 11.25; Macigno Costiero: Iv 19; Macigno del Chianti: Iv 11.5.

Data from Cornamusini, 2002; see Table 3 and Fig. 8).

c) Maestà Stratigraphic Section Sandstones of the Maestà section are included in the lobe-fringe facies (M1 and M3 samples), basin plain facies (M8 sample) and slurried divisions (M5 sample). Sandstones are quartzofeldspathic (average value: $Qm_{64}F_{30}Lt_{6}$). The average Qm/F ratio is 2.52, the highest value in the Poggio Belvedere Mb.

The overall lithic content is less abundant than the other sec- tions and the metasedimentary lithic fragments are always more abundant than the sedimentary fragments (average value: $Lm_{82}Lv_{0}Ls_{18}$; Fig. 6). Quartz grains are the most abundant constit- uents in all the studied facies and their amount reaches a large amount in laminated sandstones of lobe-fringe facies (F7 facies), sampled in the mid-top part of the section (M3 sample: Qm 79%; Qm/F 4.77). Quartz grains show high sorting and occur as sub- rounded and subspherical monocrystalline grains. Feldspars (both plagioclase and K-feldspars) are abundant, and plagioclase versus total feldspars ratio is high as well in Renali section (P/F 0.76). The few metasedimentary lithic grains include fine-grained micaschist, comprising also few chloriteschist fragments, and rare slate and phyllite. Siltstone fragments are rare or absent, whereas chert grains are present (e.g. M1 sample; F4 facies). Phaneritic fragments of plutonic rocks occur, and metamorphic fragments result to prevail in some laminate sandstones (average value $Rg_{43}Rs_{10}Rm_{47}$). Coarse gneissic fragments are rare.

Similarly to Renali area, the Maestà sandstones can be compared to both Macigno Appenninico of Northern Tuscany (Di Giulio, 1999: $Qm_{59}F_{29}Lt_{17}$; Bruni et al., 2007: average value, $Qm_{50}F_{34}Lt_{16}$) and Poggio Belvedere sandstones of Trasimeno Lake (Barsella et al., 2009: $Qm_{36\text{-}61}F_{14\text{-}24}Lt_{10\text{-}25}$) (Fig. 7), although average feldspar is considerably higher, and lithic composition is subordinate. The lithic percentage is quite similar to that reported by Cornamusini (2002) for the Macigno del Chianti in Southern

392 Tuscany ($Lm_{82}Lv_{11}Ls_{7}$), with differences in volcanic amount. These sand- stones show
393 some similar petrological characteristics with Renali sandstones excepting for average
394 lithic component and missing of volcanic grains.
395
396 *1.1. Biotic assemblage of calciturbidites*
397
398 The samples collected in graded-laminated intervals of calci- turbidites (R1 sample: F8
399 facies) (*rudstone* texture; Dunham, 1962; Embry and Klovan, 1971) comprise several mm
400 to cm-sized ? Eocene to ?Early Miocene macroforaminifers, including mainly
401 alveolinids, nummulitids and lepidocyclinids with small benthic shallow water and deep
402 water foraminifers (Fig. 7H). Extrabasinal carbonate grains are present and they include
403 biomicritic and peloidal limestones, coralline algae (*Rhodophyta*), thick shelled bi-
404 valves, echinoids and bryozoan fragments. Planktonic foraminifers (globigerinids) and
405 porcelaneous small foraminifers (miliolids), coupled with radiolarians, sponge spicules
406 and ostracods, have been recorded as mm-grained extrabasinal grains in wackestones.
407 Samples from laminated-convolute facies (R9 and R2; F9aeb) have mixed carbonate-
408 siliciclastic composition (hybrid arenites *sensu* Zuffa, 1980) with abundant skeletons of
409 bivalves and benthic foraminifers, and angular silt-size quartz and micas grains.
410
411 *1.2. Comparison with modern sand analogues*
412
413 The studied detrital modes of the Macigno Fm. can be compared with the modern
414 analogues continental and marine sands of Calabria reported from Ibbeken and
415 Schleyer (1991), Critelli and Le Pera (1994, 1998, 2003), Le Pera et al. (2001), and Perri
416 et al. (2012b) (Table 3). Valloni et al. (1991) and Di Giulio (1999) have done similar
417 studies.

In general, the average value of the Macigno Fm. sandstones ($Qm_{57}F_{34}Lt_{9}$; this study) is quite similar to the average value of modern sands of Calabria ($Qm_{51}F_{28}Lt_{21}$, Ibbeken and Schleyer, 1991) except for a visible depletion in the fine-grained lithic component. In detail, the mean of the detrital modes in sandstones of the Pianello Stratigraphic section ($Qm_{49}F_{40}Lt_{11}$, Qm/F 1.33) are comparable with granite-sourced modern sands analyzed by Ibbeken and Schleyer (1991) in which the average value is $Qm_{46}F_{33}Lt_{21}$ with a Qm/F ratio of 1.3 (see Table 3). In particular W-oriented sandstones of the outer lobe-fringe facies ($Qm_{39}F_{46}Lt_{15}$, Qm/F ¼ 0.94) are very similar with modern Calabrian sands of the Neto-Lipuda petrofacies ($Qm_{36}F_{46}Lt_{18}$, Qm/F 0.8; data reported from Le Pera et al., 2001; Perri et al., 2012b) deposited in the Ionian sea offshore that is derived from a plutonic-dominated source area (Sila Massif).

Differently from Pianello stratigraphic section, detrital modes of the Renali (average value: $Qm_{58}F_{31}Lt_{11}$, Qm/F ¼ 1.93) and the Maestà sandstones (average value: $Qm_{64}F_{30}Lt_{6}$, Qm/F 2.52) show similar petrological characteristics with granitoid plus metamorphic-sourced modern Calabrian sands ($Qm_{55}F_{24}Lt_{21}$, Qm/ F 2) reported from Ibbeken and Schleyer (1991). Thus, there is a visible depletion in felsic grains going from the Pianello toward the Renali and Maestà Stratigraphic sections (see Section 7).

2. Mineralogical and geochemical composition of mudstones

2.1. *Mineralogy of mudstones*

Whole-rock XRD analyses (Table 4) indicate that phyllosilicates are the main mineralogical components, ranging from 48% to 69% of the bulk rock. Illite and mica prevail with values up to 53%, whereas chlorite ranges from 10% to 25%. Kaolinite

445 occurs in minor amounts. Among the interstratified minerals, the IeS mixed layers are
446 slightly more abundant, but the amounts of CeS mixed layers are less abundant. The
447 non-phyllosilicate minerals are represented by quartz, feldspars (plagioclase and K-
448 feldspar) and carbonates (calcite and dolomite). Quartz ranges from 20% to 26%.The
449 amount of K-feldspar ranges up to 2%, and the amount of plagioclase ranges from a few
450 percent up to 19%. Dolomite is present in trace amounts in the PA1 and PA2 samples
451 of the Pianello sections. Calcite occurs in all samples and it ranges from few percent up
452 to 11% in the upper portion of the Pianello section and throughout the Renali section.
453 Variation of mineral concentrations is related to the different source areas that
454 influence the chemical and mineralogical composition of the sediments.
455
456 2.2. *Whole-rock geochemistry of mudstones*
457
458 Major- and trace-element concentrations are listed in Table 5. The studied mudstones
459 have been plotted in the classification di- agram for terrigenous rocks (Fig. 9). The
460 SiO_2/Al_2O_3 ratio, the most commonly used parameter, reflects the relative abundance of
461 quartz, feldspar and clay minerals (e.g., Potter, 1978). The studied samples plot in the
462 field of shale, toward the wacke field, thus reflecting variation in the
463 quartzefeldspars/mica ratio in the studied samples.
464 Geochemical compositions of the studied mud samples and the Post-Archean
465 Australian Shales (PAAS; Taylor and McLennan, 1985) were normalized to the to the
466 Upper Continental Crust (UCC; McLennan et al., 2006) (Fig. 10).
467 The mudstones are characterized by narrow compositional ranges for SiO_2, Al_2O_3,
468 MnO and K_2O, which have concentrations close to those of the UCC (Fig. 10). Sodium
469 and phosphorous are strongly depleted relatively to UCC, but CaO is variable in
470 concen- tration ranging from 1.65 (PA2) to 7.03 wt.% (PA4). The observed Na_2O
471 depletion is likely due to the burial history of these samples, which promoted the

formation of K-rich, mica-like clay minerals. The high CaO concentrations are related to the carbonate minerals present in some samples of Renali area, although the highest values of CaO have been also recorded within mudstones of Pianello area. Magnesium is enriched relatively to UCC, ranging from to 5.73 (PA2) to 9,69 wt.% (MA1), and its abundance is linked to occurrence of micas, as biotite and chlorite. Titanium and Fe_2O_3 values are also high. The general trend of the observed UCC pattern shows similar variations with those observed for the PAAS (Fig. 10).

In a ternary plot of SiO_2 (representing quartz), Al_2O_3 (repre- senting mica/clay minerals), and CaO (representing carbonates), the mudstones of Poggio Belvedere Mb. can be described as mix- tures of an aluminosilicate component with a small amount of carbonate phases (Fig. 11), although samples from Renali area and PA4 from Pianello area show higher Ca content than the average shales (PAAS).

These chemical associations and elemental variations are related to the mineralogical composition of the studied mudstones, as shown above by the mineralogical analyses.

3. Discussions

3.1. *Provenance*

Detrital signatures of the Poggio Belvedere Mb. of the Macigno Fm. contain an abundance of feldspars and coarse-grained pha- neritic rock fragments, suggesting a source area of mostly plutonic and metamorphic rocks, with minor mafic magmatic and sedi- mentary rocks. Various ratios of feldspar, lithic fragment types, and quartz types in the sandstones reflect their transition between basement uplift and a transitional continental provenance type (Figs. 6e8; e.g. Dickinson, 1985). Sandstones of the Pianello Strati- graphic section of the Macigno Fm. are richer in F than those of

498 the Renali and Maestà stratigraphic sections. The latter sections have a Q-enrichment
499 trend.

500 Referring to other diagrams, studied sandstones plot at the RgRm side in either
501 RgRvRm and RgRsRm diagrams (Critelli and Le Pera, 1994, 1995) and Lm in the
502 LmLvLs diagram, confirming a transition between plutonic and metamorphic rock
503 fragments. In detail, Pianello and Renali sandstones have an abundance of plutonic
504 rock fragments, although some samples from the Renali area have a mixture of
505 plutonic and metamorphic detritus. The Maestà sandstones plot between plutonic
506 and metamorphic rock fragment field. This indicates a slight metamorphic trend.
507 Petro- logical data indicate that sandstones of Pianello Stratigraphic sec- tion represent
508 the results of prevalent drainage from an uplifted crystalline batholith with a
509 dominance of granitoid rocks (grano- diorite and tonalite) and minor metamorphic
510 rocks (gneiss and schist) (Qm/F 1.3; e.g. Ibbeken and Schleyer, 1991), whereas
511 sandstones of the Renali and Maestà Stratigraphic sections reflect a provenance from a
512 source area with a metamorphic-dominated basement (mica-schist, fine-grained
513 schist and phyllite. Qm/ F 2; e.g. Ibbeken and Schleyer,1991). This suggests the
514 occurrence of different pathways of drainage, resulting in a variation between a plutonic
515 and metamorphic contribution and in quartz-feldspar ratio, or provenance from
516 different but similar source areas, uplif- ted in the same time span. The main source
517 area for the Macigno sandstones are inferred to be from the Western-Central Alps,
518 located north and northwest from the Macigno foreland basin system.

519 The basement of the Western-Central Alps mainly consists of continental and oceanic-
520 derived high pressure metamorphic rocks (blueschist and greenschist facies) including
521 ophiolites, marbles, calce-schists, micas-schists, limestones, marls, and crystalline
522 rocks, derived from external massifs (i.e. Monte Rosa and Gran Paradiso Massifs and
523 Dent Blanche complex). According to geological and geodynamic data, based on age
524 and amount of uplift, surface extent of source area, and volume of uplifted rocks, the li-

525 thology of eroded rocks which were transferred to the Macigno foreland basin system
526 can be inferred from the Ivrea-Verbano block (Di Giulio, 1999). Moreover the plutonic
527 component of the Macigno Fm. sandstone could be related to less uplifted South Alpine
528 crystalline basement of the Central Southern Alps (e.g. Bigi et al., 1990; Di Giulio,
529 1999). Its prevalent metamorphic composi- tion, with only minor granite intrusions, is
530 comparable with provenance constraints based on the Macigno sandstone detrital modes
531 (average value $Qm_{54}F_{29}Lt_{17}$; Qm/F 1.9) studied in previous works (e.g. Di Giulio,
532 1999). The compositional results closely correspond with detrital modes reported in
533 overall sandstones of Poggio Belvedere Mb. of the present study (average value:
534 $Qm_{57}F_{34}Lt_{9}$; Qm/F 1.85), suggesting a general provenance from northwestward Alpine
535 metamorphic-dominated domains. The occurrence of a volcanic signal, and sedimentary
536 detritus, could be inferred from ophiolites and their sedimentary cover of Ligurian
537 Nappe, although some volcanic grains, which have felsic granular texture with
538 plagioclase phenocrysts, might also indicate a prove- nance from calc-alkaline trend
539 volcanic arcs (i.e. Corsica-Sardinia block, Cornamusini et al., 2002).

540 The W-oriented granitic-sourced sandstones of the Pianello area testify to the
541 influence of terrigenous material coming from a westernmost source area. The
542 composition of these sandstones could correspond with source rocks of the Corsica-
543 Sardinia block as Cornamusini et al. (2002) reported for the "Macigno Costiero"
544 Fm. However, the minor content of volcanic lithic fragments, less abundant than in
545 the "Macigno Costiero" Fm., and the location of Corsica-Sardinia during Late
546 Oligocene-Early Miocene, which was relatively far from Umbria-Tuscany foreland
547 basin system (Guerrera et al., 2015), also indicate the Alpine chain as W-derived
548 crystalline source area (Fig. 12). The provenance of plutonic- dominated sandstones
549 from the less uplifted Central Alps crystalline basement, located northwestward, do
550 not explain the large amount of feldspars and phaneritic plutonic rock fragments (e.g.
551 Pianello Stratigraphic section), which are clearly more abundant than other

552 sandstones collected in the Macigno Apenninico (Valloni et al., 1991; Di Giulio,
553 1999; Dinelli et al., 1999; Cornamusini, 2002; Barsella et al., 2009). In detail, the
554 distance between the Central Alpine crystalline basement and the Macigno basin of
555 Trasimeno Lake area in the reconstructed palaeogeo- graphic framework (Fig. 12) is
556 estimated to be several hundred of kilometres. We suggest a provenance from
557 Mesomediterranean terranes that were close to the basin. To support this conclusion, the
558 Pianello lobe-fringe sandstones (F4 to F7 facies; Mutti, 1992), with the contribution
559 of sudden decelerations of mud-rich turbidity currents (Type 1 Beds by Tinterri and
560 Muzzi-Magahalaes, 2011), represent the final result of depositional processes starting
561 from a plutonic-dominated source area that were very close to the Macigno foreland
562 basin. The granite-sourced sandstones of Pianello area is inferred to have been derived
563 by drainage of the Monte Rosa and Gran Paradiso massifs and Dent Blanche complex,
564 located westward from the palaeo-Alps (Fig. 12), in which zircon fission- track ages
565 of exhumation (related to almost 40 ma) are closely related with those of the
566 Macigno sandstones (Dunkl et al., 2001) The subordinate presence of extrabasinal
567 carbonate detritus (e.g. Zuffa, 1985; Critelli et al., 2007) may suggests an additional
568 source area composed of ?Eocene to early Miocene limestones, as shown by
569 extrabasinal carbonate grains and fossils in the calci- turbidites of the Renali area.
570 The occurrence of benthic macro- forams suggests a provenance from an external
571 shelf environment, but wackestone-texture clasts including planktonic foraminifers
572 (*globigerinids*) indicate a clear signal from an inner basin. Similar biofacies have
573 been distinguished within calciturbidite and breccia levels of the Eocene-Oligocene
574 Scaglia Toscana Fm. in the Chianti Hills area, in which traction features indicate
575 palaeoflows towards the S and SW (Ielpi and Cornamusini, 2013) suggest a
576 provenance from the Adria margin.

577 The variation among the LREEs (Light Rare Earth Elements; e.g.,
578 La and Ce) and the transition elements (e.g., Co, Cr and Ni) is considered a useful

579 indicator in provenance studies (e.g., Culler, 2000; Perri et al., 2012b). The range of
580 elemental ratios (LaþCe/
581 Co, LaþCe/Cr, and LaþCe/Ni; Table 5) of all samples studied sug
582 gests a provenance from fairly felsic rather than mafic source-areas (e.g., Perri et al.,
583 2012b). These ratio values do not exclude a supply of a mafic source, predominantly for
584 the Maestà section that shows lower La Ce/Cr (on average 0.47) and La Ce/Ni (on
585 average 0.79) than those of the Pianello and Renali sections (Table 5).
586 Generally, a low concentration of Cr and Ni indicates sediments derived from a felsic
587 provenance, whereas, higher content of these elements are mainly found in sediments
588 derived from ultramafic rocks (e.g., Wrafter and Graham, 1989; Armstrong-Altrin et al.,
589 2004). Furthermore, the Cr/V ratio is an index of the enrichment of Cr over the other
590 ferromagnesian trace elements, whereas Y/Ni monitors the general level of
591 ferromagnesian trace elements (Ni) compared to a proxy for the HREE (Y).
592 Maficeultramafic sources tend to have high ferromagnesian abundances; such a
593 provenance would result in a decrease in Y/Ni ratios and an increase in Cr/V ratios (e.g.,
594 Hiscott, 1984; McLennan et al. 1993). The Cr/V *vs.* Y/Ni diagram (Hiscott, 1984)
595 indicates a mixed source for the studied samples. In particular, the sediments are derived
596 from a mainly felsic source area with a supply of a mafic source, predominantly for the
597 Maestà section that shows Cr/V values ranging from 1.15 to 3.36 (Fig. 13). The
598 VeNieLa*10 diagram also suggests a similar prove- nance (e.g. Bracciali et al., 2007; Perri
599 et al., 2011b) (Fig. 14), where the studied samples fall in an area related to provenance
600 from a mixed source, mainly characterized by felsic rocks with a supply of mafic rocks.
601 The mafic supply is probably related to the Ligurian ophiolites.

602 *3.2. Source-area weathering*

603 The evaluation of the source area weathering processes is mainly related to the
604 variation of alkali and alkaline-earth elements in siliciclastic sediments. The Chemical

605 Index of Alteration (CIA; Nesbitt and Young, 1982) is one of the most used indices to
606 quantify the degree of source area weathering. Furthermore, when the sediments
607 contain a high proportion of CaO, an alternative index of alteration CIA', expressed
608 as molar volumes of [Al/ (Al Na K)] 100, has also used (e.g., Perri et al.,
609 2014, 2015). The chemical compositions of studied mudstones are plotted as molar
610 proportions within the AeCNeK and AeNeK diagrams. The CIA values of the
611 studied samples are quite homogeneous (average 66.4) with low-moderate values
612 and in the AeCNeK triangular diagram the samples plot in a tight group on the A-K
613 join close to the illite-muscovite point (Fig. 15A), suggesting low- moderate
614 weathering conditions. Furthermore, the CIA' values of the mudrocks (average 69.7)
615 are quite similar to the CIA, typical of low-moderate weathering conditions. In the
616 AeCNeK triangular diagram the samples plot in a tight group on the A-K join close to
617 the illite-muscovite point (Fig. 15B). Micas (both illite and musco- vite) are the
618 dominant phyllosilicates occurring within the studied mudstones.
619 Simple ratios such as Al/K and Rb/K (e.g., Schneider et al.,
620 1997; Roy et al., 2008), characterized by elements with con- trasting mobility in the
621 supracrustal environment, have been also used as a broad measure of weathering.
622 Generally, high Al/K ra- tios are typical of sediments enriched in kaolinite, an
623 important product of intensive weathering, over feldspar (or other K- bearing
624 minerals). The Al/K ratios are low and constant (average 4.47 ± 0.41) for all the
625 studied sediments suggesting low-moderate weathering and no important fluctuations
626 in weathering intensity, as also shown in the AeCNeK and AeNeK diagrams (Fig. 15).
627 Furthermore, Rb/K ratios have been used to monitor source area weathering, where K
628 is preferentially leached over Rb with increased intensity of weathering (Wronkiewicz
629 and Condie, 1989, 1990; Peltola et al., 2008). Very low and homogeneous values of
630 Rb/K ratios (<0.006) are found in the studied sediments, indicating weak to moderate
631 weathering in a warm-humid climate (typical of the Mediterranean area) with

minimal or negligible variations over time (e.g., Mongelli et al., 2012 and references therein).

1.1. *Sorting, transport and recycling*

Generally, transport and deposition of terrigenous sediments involve mechanical sorting, that may affect the chemical compo- sition of terrigeneous sediments and, thus, the distribution of source area weathering and provenance proxies (e.g., Mongelli et al., 2006; Perri et al., 2011a, 2012a, 2014).

Aluminum, titanium and zirconium are the major and minor elements generally considered the least mobile during chemical weathering (e.g. Perri et al., 2008a). Resistant minerals such as zircon, rutile and ilmenite generally host significant amounts of Ti and Zr. Variations in these elements are expressed in the AleTieZr ternary plot (García et al., 1994) that can highlight the possible effect of zircon addition mainly related to sorting and recycling processes. The studied mudstones plot in a tight area in the middle of the 15*Al_2O_3eZr-300*TiO_2 diagram (Fig. 16), and they are mostly characterized by homogeneuos values in the Al_2O_3/Zr ratio that could be due to poor recycling effects without a marked Zr enrichment (e.g., Perri et al., 2008a, 2011a; Caracciolo et al., 2011 and references therein).

The Index of Compositional Variability (Cox et al., 1995) has been generally used as a measure of compositional maturity. Immature mudstones, containing a high proportion of silicates other than clays, commonly show high values of this index (ICV>1), whereas mature mudstones, depleted in silicates other than clays, generally show low ICV values (ICV<1). Furthermore, immature mudrocks tend to be found in tectonically active settings and are character- istically first-cycle deposits (Van de Kamp and Leake, 1985), whereas mature mudrocks characterize tectonically quiescent or cratonic environments (Weaver, 1989) where sediment

658 recycling is active. The studied sediments show ICV>1 (average 1.51 ± 0.26) typical of
659 first cycle, immature sediments where chemical weath- ering plays a minor role
660 consistent with the medium-low CIA and CIA' values. Furthermore, the ICV values are
661 also consistent with the sample distribution within the AleTieZr ternary plot that
662 exclude recycling effects for the studied sediments, suggesting a very rapid transport in
663 a depositional area close to the source(s). Such geochemical interpretation is totally
664 compatible with ichnocoe- nosis, reported by Monaco and Trecci (2014). In fact the
665 very large abundance of endichnial *Halopoa* (*H. embricata* and *H.* var. *fucu- sopsis*)
666 suggests a basin floor environment rich in organic matter (i.e. phyto detritus) and
667 diversified geochemical elements, extremely important to a proliferation of this
668 ichnotaxon close to an alimentation source. Moreover the missing of *Avetoichnus*
669 *luisae*, *Zoophycos* and *Nereites* trace fossils (see the ichnosubfacies at *Nereites*),
670 occurring in the underlying Scaglia Toscana Fm. and in the overlying Marnoso Arenacea
671 Fm., typical of distal deep-water areas, testifies to a very high sedimentation rate and
672 the proximity of the depositional area to the source area. The differences among ich-
673 notaxa is minimal in the three studied stratigraphic sections. However a slightly
674 increasing on graphoglyptid abundance and diversification can be noted in the upper
675 Renali and Maestà sec- tions differently to the Pianello section (e.g. *Paleodictyon* and
676 *Spi- rorhaphe*). This could be explained due to a progressive deepening of the basin
677 plain environment.

678 The textural characteristics of the studied sandstones show moderate to low sorting, low
679 degree of roundness of grains, and lack of altered quartz grains, confirming either poor
680 recycling or closeness to the source area. However, sandstones at the Maestà
681 Stratigraphic section are well sorted, indicating the settling of a fine-grained turbidite
682 flow (F9 facies) in farthermost portion of the foredeep basin. Furthermore, the good
683 sphericity of some clasts, their general equant-prolate shape, and their poor degree of flat-
684 tering in outer lobe facies (F5eF7 facies in Pianello and Renali Stratigraphic sections)

685 suggest that grains were initially reworked in a deltaic/fluvial sedimentary system and
686 then resedimented into a deep-sea basin (e.g. Sames,1966; Walker,1975). Finally in Pianello
687 Stratigraphic section the occurrence of well preserved continental vegetal remains and
688 several slurried divisions indicate fast and sudden transport (e.g. hyperpicnal plumes),
689 from a close source area which were more probably located westward, as well indi-
690 cated by W-oriented sandy debris flows.
691
692 ## 4. Conclusions
693
694 The Macigno Fm. sandstones, sampled in Poggio Belvedere Mb. in the Trasimeno
695 Lake area, show a general quartzofeldspathic composition, but with some differences in
696 the quartz/feldspar ratio (Qm/F) and in the composition of either phaneritic rock
697 fragments and fine-grained lithic fraction.
698 The abundance of feldspars (lower Qm/F) and phaneritic plutonic and discrete
699 occurrence of high-grade metamorphic rock fragments in lobe-fringe facies sandstones
700 (F5eF7 facies) of the Pianello Stratigraphic section match those found in some granitoid-
701 source modern sands of Calabria (Ibbeken and Schleyer, 1991; Perri et al., 2012b). These
702 data, coupled with evidence of W-oriented flows, suggest a provenance from a granitoid-
703 dominated batholith, and indicate the external massifs of the Western Alps (Monte Rosa
704 and Gran Paradiso massifs, Dent Blanche complex) as a potential plutonic and high-
705 grade metamorphic source area.
706 The overall NWeSE oriented fine-grained turbidites of the basin plain facies (F8 and
707 F9a-b facies) and lobe-fringe sandstones of the Maestà Stratigraphic section have a higher
708 Qm/F ratio than those of Pianello Stratigraphic section. They are characterized by a
709 lower plutonic content, metamorphic lithic fragments, a fine-grained, low-medium grade
710 metamorphic component, and subordinate volcanic lithic fragments in a similar amount
711 with those studied previously in the sandstones of the Macigno Fm. (Di Giulio et al.,

712 1999 and Barsella et al., 2009) and in metamorphic-source mod- ern sands of Calabria
713 (Ibbeken and Schleyer, 1991). These data mainly suggest a provenance from a
714 metamorphic basement and a crystalline batholith that can be respectively identified
715 with the IvreaeVerbano block in Central-Western Alps and South Alpine crystalline
716 basement in the Central Southern Alps (Di Giulio, 1999). Volcanic and metavolcanic
717 grains, coupled with Cr and Ni enrichment, mainly indicate a provenance from an
718 ophiolitic unit and overlying sedimentary cover of the Ligurian Nappe. An enrichment
719 of Nb and a peculiar occurrence of volcanic fragments with felsic granular fabric
720 including plagioclase and quartz phe- nocrysts could be related to calco-alkaline
721 rhyolites which char- acterize the Late Oligo-Early Miocene volcanic arc that originated
722 by subduction of the Adria microplate beneath the eastern margin of Mesomediterranean
723 continent (Guerrera et al., 2015). Finally the presence of East-derived calciturbidites in the
724 Renali area including
725 a typical biofacies of external shallow-water platform.
726 This detailed petrology coupled with sedimentological data (Monaco and Trecci, 2014)
727 allows a better understanding of the spatial compositional evolution of the Macigno Fm.,
728 in agreement with the model for migrating foredeep basins proposed by Ricci Lucchi
729 (1986). Firstly sedimentation developed in the western- most internal zones, which were
730 transversally fed mainly by the crystalline basement of external massifs. During the
731 migration of the orogenetic front and foredeep basin, the transversal feeders were
732 substituted by longitudinal basin feeders from Western- Central Alps that were supplied
733 with material similar to those from external massifs but with minor plutonic and high-
734 grade metamorphic fragments. In the Late OligoceneeEarly Miocene time interval, the
735 Trasimeno Lake area was probably located in the distal external zones of Macigno
736 foredeep that received terrigenous material firstly from the WeSW-oriented external
737 massifs feeders (Pianello and lower Renali areas) and successively from the NW-
738 oriented Central Alpine and S-oriented Apennine feeders (upper Renali and Maestà

739 areas). Also ichnocoenoses seem to confirm this evolutionary trend. A similar
740 compositional trend could be accounted for the Macigno Fm. in Northwestern Tuscany
741 (Abetone area) analyzed by Bruni et al. (2007).

742 The geochemistry and mineralogy of Late OligoceneeEarly Miocene deep-sea
743 mudstones from Poggio Belvedere stratigraphic section of the Macigno Fm. suggest
744 interesting palaeoclimatic and paleoweathering indications. The mudrocks have
745 concentrations very similar to those of the UCC (McLennan et al., 2006) for Si, Al, Fe,
746 Zr, K, whereas, Ca, Na, P, Ba and Sr are strongly depleted. Cesium and rubidium are
747 slight enriched to the UCC and show a positive correlation with potassium, suggesting
748 these trace elements are mostly hosted by dioctahedral mica-like clay minerals. This in
749 turn indicates that illite and illitic minerals (I/S mixed layers) have played an important
750 role in the distribution of elements in these rocks since these minerals are abundant in
751 the studied samples. Furthermore, the mudstones fall in a tight group on the AeK join,
752 in the AeCNeK triangular diagram, close to the muscovite point, in agreement with the
753 mineralogical data. The Cr, Ni and Nb con- centrations are enriched to the UCC, and
754 indicate a trace of a mafic source.

755 The source area for the studied mudstones should have similar
756 features to those of Western-Central Alps and crystalline external massifs basement,
757 which are predominantly composed of felsic rocks with non-trivial amounts of mafic
758 rocks. Geochemical proxies consistently suggest a felsic nature of the source area, with
759 a minor but not negligible supply from mafic rocks that increased in the younger
760 deposits (Maestà Stratigraphic section).

761 Both the CIA and the CIA' proxies suggest low-moderate weathering at the source
762 area. The studied sediments seems to be affected by brief reworking in fluvial/deltaic
763 zone and poor recy- cling processes and, as a consequence, it is likely these proxies
764 monitor cumulative effects of weathering (e.g., Mongelli et al., 2006; Critelli et al.,
765 2008; Perri et al., 2008a, 2008b).

The chemical weathering of such rocks under a humid climate season would produce an initial illitization of silicate minerals. Moreover, palaeocurrent analysis clearly indicates that terrigenous rocks derived from rapid erosion of highlands located to the N, NW, W and E of the present-day outcrops of the Trasimeno Lake area.

Acknowledgements

U. Amendola was supported by the “;CARICAL Fundation”; in Cosenza, Italy. Work supported by the MIUR-UNICAL Project (Re- lationships between Tectonic Accretion, Volcanism and Clastic Sedimentation within the Circum-Mediterranean Orogenic Belts, 2006e2011; Resp. S. Critelli). We are grateful to reviewers Manuel Martín-Martín, an anonymous reviewer and the Associate Editor Massimo Zecchin for reviews, helpful discussions, and comments on an earlier version of the manuscript.

References

Andreozzi, M., Di Giulio, A., 1994. Stratigraphy and petrography of the M. Cervarola sandstones in the type area, Modena Province. Mem. Soc. Geol. It. 48, 351e360. Armstrong-Altrin, J.S., Lee, Y.I., Verma, S.P., Ramasamy, S., 2004. Geochemistry of sandstones from the upper miocene kudankulam Fm., southern India: impli- cations for provenance, weathering, and tectonic setting. J. Sed. Res. 74,
285e297. http://dx.doi.org/10.1306/082803740285.
Aruta, G., 1994. Stratigraphy of the falterona and cervarola sandstones in the cor-
tona area (Arezzo, northern Apennines). Mem. Soc. Geol. It. 48, 361e369. Aruta, G., Pandeli, E., 1995. Lithostratigraphy of the m. Cervarola e m. Falterona Fm. between Arezzo and trasimeno Lake (Tuscan-Umbria, northern apennines,
Italy). Giorn. Geol. 57 (1e2), 131e157 serie 3a.

792 Aruta, G., Bruni, P., Cipriani, N., Pandeli, E., 1998. The siliciclastic turbidite sequences
793 of the tuscan domain in the val di Chiana-Val Tiberina area (eastern Tuscany
794 and north-western Umbria). Mem. Soc. Geol. It. 52, 579e593.
795 Barsella, M., Boscherini, A., Botti, F., Marroni, M., Meneghini, F., Motti, A., Palandri, S., Pandolfi,
796 L., 2009. Oligocene-Miocene foredeep deposits in the Lake Trasimeno area (Central Italy): insights
797 into the evolution of the northern Apennines. Ital. J. Geosci. Boll. Soc. Geol. It.) vol. 128 (No. 2),
798 341e352. http://dx.doi.org/10.3301/
799 IJG.2009.128.2.341.
800 Basu, A., 1985. Reading provenance from detrital quartz. In: Zuffa, G.G. (Ed.),
801 Provenance of Arenites. D. Reidel Publishing, Boston, pp. 231e247.
802 Bauluz, B., Mayayo, M.J., Fernandez-Nieto, C., Gonzalez Lopez, J.M., 2000. Geochemistry of
803 precambrian and paleozoic siliciclastic rocks from the Iberian range (NE Spain): implications for
804 source-area weathering, sorting, provenance, and tectonic setting. Chem. Geol. 168, 135e150.
805 http://dx.doi.org/10.1016/
806 S0009-2541(00)00192-3.
807 Bigi, G., Castellarin, A., Coli, M., Dal Piaz, G.V., Sartori, R., Scandone, P., Vai, G.B., 1990.
808 Structural Model of Italy, Scale 1:500,000, Sheet N. 1. S.E.L.C.A. press, Florence. Boccaletti, M.,
809 Calamita, F., Deiana, R., Gelati, R., Massari, F., Moratti, G., Ricci Lucchi, F., 1990. Migrating
810 foredeep-thrust belt system in the northern Apen- nines and southern Alps. Palaeogeogr.
811 Palaeoclimatol. Palaeoecol. 77, 3e14.
812 http://dx.doi.org/10.1016/S0009-2541(00)00192-3.
813 Bracciali, L., Marroni, M., Luca, P., Sergio, R., 2007. Geochemistry and petrography of
814 western tethys cretaceous sedimentary covers (Corsica and Northern Apen- nines): from source
815 areas to configuration of margins. GSA Spec. Pap. 420, 73e93.
816 http://dx.doi.org/10.1130/2006.2420(06).

817 Brozzetti, F., 2007. The Umbria Preapennines in the Monte Santa Maria Tiberina area: a new
818 geological map with stratigraphic and structural notes. Boll. Soc. Geol. It. 126 (3), 511e529.
819 Bruni, P., Pandeli, E., 1980. Torbiditi calcaree nel Macigno e nelle Arenarie del Cer- varola
820 nell'area del Pratomagno e del Falterona (Appennino settentrionale). Mem. Soc. Geol. It. 21,
821 217e230.
822 Bruni, P., Pandeli, E., Nebbiai, M., 2007. Petrographic analysis in regional geology interpretation:
823 case history of the Macigno (northern Apennines). In: Arribas, J., Critelli, S., Johnsson, M. (Eds.),
824 Sedimentary Provenance: Petrographic and Geochemical Perspectives, Geological Society of
825 America Special Paper 420, pp. 95e105. http://dx.doi.org/10.1130/2006.2420(07).
826 Canuti, P., Focardi, P., Sestini, G., 1965. Stratigrafia, correlazione e genesi degli Scisti Policromi
827 dei monti del Chianti (Toscana). Boll. Soc. Geol. It. 84, 93e166.
828 Caracciolo, L., Le Pera, E., Muto, F., Perri, F., 2011. Sandstone petrology and mudstone
829 geochemistry of the PeruceKorycany Fm. (Bohemian cretaceous Basin, Czech Republic). Int. Geo.
830 Rev. 53, 1003e1031. http://dx.doi.org/10.1080/ 00206810903429011.
831 Castellarin, A., 1992. Introduzione alla progettazione del profilo CROP. Studi Geol. Camerti, Spec.
832 1992 (2), 9e15.
833 Cavalcante, F., Fiore, S., Lettino, A., Piccarret, G., Tateo, F., 2007. Illiteesmective mixed layers in
834 silicide shales and piggy-back deposits of the Gorgoglione Fm. (Southern Apennines): geological
835 inferences geodynamic implications. Bol. Soc. Geol. It 126, 241e254.
836 Centamore, E., Fumanti, F., Nisio, S., 2002. The Central northern apennines geological evolution
837 from Triassic to Neogene time. Boll. Soc. Geol. It., Spec. 1, 181e197.
838 Condie, K.C., Noll, P.D.J., Conway, C.M., 1992. Geochemical and detrital mode evi- dence for-
839 twosourcesofearlyProterozoicsedimentaryrocksfromtheTontoBasinSupergroup, central Arizona.
840 Sed. Geol. 77, 51e76. http://dx.doi.org/10.1016/0037-0738(92) 90103-X.
841 Condie, K.C., Lee, D., Farmer, G.L., 2001. Tectonic setting and provenance of the Neoproterozoic
842 uinta mountain and Big Cottonwood groups, northern Utah: constraints from geochemistry, Nd

843 isotopes, and detrital modes. Sed. Geol. 141, 443e464. http://dx.doi.org/10.1016/S0037-
844 0738(01)00086-0.
845 Cornamusini, G., 2002. Compositional evolution of the Macigno Fm. of southern Tuscany along a
846 transect from the Tuscan coast to the Chianti Hills. Boll. Soc. Geol. It. 1, 365e374.
847 Cornamusini, G., Elter, F.M., Sandrelli, F., 2002. The CorsicaeSardinia Massif as source area for
848 the early northern Apennines foredeep system: evidence from debris flows in the “Macigno
849 costiero” (Late Oligocene, Italy). Int. J. Earth Sci. Geol. Rundsch) 91, 280e290.
850 http://dx.doi.org/10.1007/s005310100212.
851 Cox, R., Lowe, D., Cullers, R.L., 1995. The influence of sediment recycling and basement
852 composition on evolution of mudrock chemistry in southwestern United States. Geochim.
853 Cosmochim. Acta 59, 2919e2940. http://dx.doi.org/ 10.1016/0016-7037(95)00185-9.
854 Critelli, S., 1993. Sandstone detrital modes in the Paleogene Liguride Complex, accretionary wedge
855 of the Southern Apennines (Italy). J. Sed. Res. 63, 464e476. http://dx.doi.org/10.1306/D4267B27-
856 2B26-11D7-8648000102C1865D.
857 Critelli, S., 1999. The interplay of lithospheric flexure and thrust accomodation in forming
858 stratigraphic sequences in the southern Apennines foreland basin system, Italy. Accad. Naz. dei
859 Lincei Rendiconti Lincei Sci. Fis. Nat. 10, 257e326.
860 Critelli, S., Ingersoll, R.V., 1995. Interpretation of neovolcanic versus palaeovolcanic sand grains:
861 an example from Miocene deep-marine sandstone of the Topanga group (southern California).
862 Sedimentology 42, 783e804. http://dx.doi.org/ 10.1111/j.1365-3091.1995.tb00409.x.
863 Critelli, S., Le Pera, E., 1994. Detrital modes and provenance of Miocene sandstones and modern
864 sands of the southern Apennines thrust-top basins (Italy). J. Sed. Res. 64, 824e835.
865 Critelli, S., Le Pera, E., 1995. Tectonic evolution of the southern Apennines thrust- belt (Italy) as
866 reflected in modal compositions of Cenozoic sandstone. J. Geol. 103, 95e105.
867 Critelli, S., Le Pera, E., 1998. Post-Oligocene sediment dispersal systems and unroofing history of
868 the Calabrian Microplate, Italy. Int. Geol. Rev. 48, 609e637. Critelli, S., Le Pera, E., 2003.

869 Provenance relations and modern sand petrofacies in an uplifted thrust-belt, northern Calabria, Italy.
870 In: quantitative provenance studies in Italy. In: Valloni, R., Basu, A. (Eds.), Servizio Geologico
871 Nazionale, Memorie Descrittive Della Carta Geologica D'Italia, 61, pp. 25e39.
872 Critelli, S., De Rosa, R., Platt, J.P., 1990. Sandstone detrital modes in the Makran
873 accretionary wedge, southwest Pakistan: implications for tectonic setting and long-distance turbidite
874 transportation. Sed. Geol. 68, 241e260. http:// dx.doi.org/10.1016/0037-0738(90)90013-J.
875 Critelli, S., Le Pera, E., Galluzzo, F., Milli, S., Moscatelli, M., Perrotta, S., Santantonio, M., 2007.
876 Interpreting siliciclastic-carbonate detrital modes in Foreland Basin Systems: an example from
877 Upper Miocene arenites of the Central Apennines, Italy. In: Arribas, J., Critelli, S., Johnsson, M.
878 (Eds.), Sedi- mentary Provenance: Petrographic and Geochemical Perspectives, GSA Special Paper
879 420, pp. 107e133. http://dx.doi.org/10.1130/2006.2420(08).
880 Critelli, S., Mongelli, G., Perri, F., Martin-Algarra, A., Martin-Martin, M., Perrone, V., Dominici,
881 R., Sonnino, M., Zaghloul, M.N., 2008. Compositional and geochemical signatures for the
882 sedimentary evolution of the Middle TriassiceLower Jurassic continental redbeds from western-
883 central Mediterranean Alpine chains. J. Geol. 116, 375e386. http://dx.doi.org/10.1086/588833.
884 Cullers, R.L., 2000. The geochemistry of shales, siltstones and sandstones of Penn-
885 sylvanianePermian age, Colorado, USA: implications for provenance and metamorphic studies.
886 Lithos 51, 181e203.
887 Damiani, A.V., Faramondi, S., Nocchi-Lucarelli, M., Pannuzi, L., 1987. Bio- cronostratigrafia delle
888 unita litologiche costituenti “l’insieme varicolore” affiorante tra la Val di Chiana ed il fiume
889 Tevere (Italia centrale). Boll. Serv. Geol. d’It. Roma 106, 109e160.
890 Di Giulio, A., 1999. Mass transfer from the Alps to the Apennines: volumetric constraints in the
891 provenance study of the MacignoeModino sourceebasin system, ChattianeAquitanian, northwestern
892 Italy. Sed. Geol. 124, 69e80. http:// dx.doi.org/10.1016/S0037-0738(98)00121-3.
893 Dickinson, W.R., 1970. Interpreting detrital modes of greywacke and arkose. J. Sed. Petr. 40,
894 695e707.

Dickinson, W.R., 1985. Interpreting provenance relations from detrital modes of sandstones. In: Zuffa, G.G. (Ed.), Provenance of Arenites, North Atlantic Treaty Organization Advanced Study Institute Series, 148. D. Reidel, Dordrecht, The Netherlands, pp. 331e361. http://dx.doi.org/10.1007/978-94-017-2809-6.

Dinelli, E., Lucchini, F., Mordenti, A., Paganelli, L., 1999. Geochemistry of Oligoce- neeMiocene sandstones of the northern Apennines (Italy) and evolution of chemical features in relation to provenance changes. Sed. Geol. 127, 193e207. http://dx.doi.org/10.1016/S0037-0738(99)00049-4.

Dunham, R.J., 1962. Classification of carbonate rocks according to depositional texture. In: Ham, W.E. (Ed.), Classification of Carbonate Rocks, AAPG Memoir. 1, pp. 108e121.

Dunkl, I., Di Giulio, A., Kuhlemann, J., 2001. Combination of single-grain fission- track chronology and morphological analysis of detrital zircon crystals in provenance studies-sources of the Macigno Fm. (Apennines, Italy). J. Sed. Res. 71 (4), 516e525. http://dx.doi.org/10.1306/102900710516.

Einsele, G., 1991. Submarine mass flow deposits and turbidites. In: Einsele, G., Ricken, W., Seilacher, A. (Eds.), Cycles and Events in Stratigraphy. Springer, Berlin, pp. 313e339.

Embry III, A.F., Klovan, J.S., 1971. A late devonian reef tract on northeastern Banks Island, N.W.T. Bull. Can. Petrol. Geol. 4, 730e781.

Flanagan, F.J., 1976. Descriptions and Analyses of Eight New USGS Rock Standards, p. 192. U.S. Geological Survey Professional Paper 840, Washington.

Folk, R.L., 1968. Petrology of Sedimentary Rocks. University of Texas Publication, Austin, p. 170.

Gandolfi, G., Paganelli, L., Zuffa, G.G., 1983. Petrology and dispersal pattern in the Marnoso-arenacea Fm. (Miocene, Northerh Apennines). J. Sed. Petr 53, 493e507. http://dx.doi.org/10.1306/212F8215-2B24-11D7-8648000102C1865D.

García, D., Fonteilles, M., Moutte, J., 1994. Sedimentary fractionations between Al, Ti, and Zr and the genesis of strongly peraluminous granites. J. Geol. 102, 411e422. Gazzi, P., 1966. Le arenarie del Flysch sopracretaceo dell'Appennino modenese;

921 correlazioni con il Flysch di Monghidoro. Miner. Petrografica Acta 12, 69e97. Graham, S.A.,
922 Ingersoll, R.V., Dickinson, W.R., 1976. Common provenance for lithic grains in carboniferous
923 sandstones from ouachita mountains and black warrior basin. Jour. Sed. Petrol. 46, 620e632.
924 http://dx.doi.org/10.1306/212F7009-2B24-
925 11D7-8648000102C1865D.
926 Guerrera, F., Martín-Algarra, A., Martín-Martín, M., 2012a. Tectono-sedimentary
927 evolution of the "Numidian Formation" and Lateral Facies (southern branch of the western Tethys):
928 constraints for centralwestern Mediterranean geo- dynamics. Terra Nova 24, 34e41.
929 Guerrera, F., Tramontana, M., Donatelli, U., 2012b. Space/time tectono-sedimentary evolution of
930 the umbria -Romagna-Marche miocene Basin (North apennines, Italy). Swiss J. Geosci. 105,
931 325e341.
932 Guerrera, F., Martin-Martin, M., 2014. Geodynamic events reconstructed in the Betic, Maghrebian,
933 and Apennine chains (central-western Tethys). Bull. Soc. Ge□ol Fr. 185, 329e341.
934 Guerrera, F., Martìn-Martìn, M., Raffaelli, G., Tramontana, M., 2015. The Early Miocene "Bisciaro
935 volcaniclastic event" (northern Apennines, Italy): a key study for the geodynamic evolution of the
936 central-western Mediterranean. Int. J. Earth Sci. Geol. Rundsch) 104, 1083e1106.
937 http://dx.doi.org/10.1007/s00531- 014-1131-5.
938 Herron, M.M., 1988. Geochemical classification of terrigenous sands and shales from core or log
939 data. J. Sed. Petr. 58, 820e829. http://dx.doi.org/10.1306/212F8E77- 2B24-11D7-
940 8648000102C1865D.
941 Hill, K.C., Hayward, A.B., 1988. Structural constraints on the Tertiary plate tectonic evolution of
942 Italy. Mar. Pet. Geol. 5, 2e16. http://dx.doi.org/10.1016/0264- 8172(88)90036-0.
943 Hiscott, R.N., 1984. Ophiolitic source rocks for Taconic-age flysch: trace element evidence. Geol.
944 Soc. Am. 95, 1261e1267. http://dx.doi.org/10.1130/0016- 7606(1984)95<1261:OSRFTF>2.0.CO;2.
945 Ibbeken, H., Schleyer, R., 1991. Source and Sediment. A Case Study of Provenance and Mass
946 Balance at an Active Plate Margin (Calabria, Southern Italy). Springer, Berlin.

947 Ielpi, A., Cornamusini, G., 2013. An outer ramp to basin plain transect: interacting pelagic and
948 calciturbidite deposition in the EoceneeOligocene of the Tuscan Domain, Adria Microplate (Italy).
949 Sed. Geol. 294, 83e104. http://dx.doi.org/ 10.1016/j.sedgeo.2013.05.010.
950 Ingersoll, R.V., Suczek, C.A., 1979. Petrology and provenance of Neogene Sand from Nicobarand
951 Bengalfans, DSDP sites 211and 218. J. Sed. Petr. 49, 1217e1228.
952 http://dx.doi.org/10.1306/212F78F1-2B24-11D7-8648000102C1865D.
953 Ingersoll, R.V., Bullard, T.F., Ford, R.L., Grimm, J.P., Pickle, J.D., Sares, S.W., 1984. The effect of
954 grain size on detrital modes: a test of the GazzieDickinson point- counting method. J. Sed. Petr. 54,
955 103e116. http://dx.doi.org/10.1306/ 212F83B9-2B24-11D7-8648000102C1865D.
956 Johnsson, M.J., 1993. The system controlling the composition of clastic sediments. In: Johnsson,
957 M.J., Basu, A. (Eds.), Processes Controlling the Composition of Clastic Sediments: GSA Special
958 Paper, 284, pp. 1e19. http://dx.doi.org/10.1130/ SPE284-p1.
959 Krumm, S., 1996. WINFIT 1.2: version of November 1996 (The Erlangen geological and
960 mineralogical software collection) of “WINFIT 1.0: a public domain program for interactive
961 profile-analysis under WINDOWS. In: XIII Conference on Clay Mineralogy and Petrology, Praha,
962 1994: Acta Universitatis Carolinae Geologica, 38, pp. 253e261.
963 Le Pera, E., Arribas, J., Critelli, S., Tortosa, A., 2001. The effects of source rocks and chemical
964 weathering on the petrogenesis of siliciclastic sand from the Neto river (Calabria, Italy):
965 implications for provenance studies. Sedimentology 48, 357e378.
966 McLennan, S.M., Hemming, D.K., Hanson, G.N., 1993. Geochimical aproaches to sedimentation,
967 provenance and tectonics. Geol. Soc. Am. Spec. Pap. 284, 21e40. McLennan, S.M., Taylor, S.R.,
968 Hemming, S.R., 2006. Composition, differentiation, and evolution of continental crust: constraints
969 from sedimentary rocks and heat flow. In: Brown, M., Rushmer, T. (Eds.), Evolution and
970 Differentiation of the
971 Continental Crust. Cambridge University Press, Cambridge, pp. 92e134. Milighetti, M., Monaco,
972 P., Checconi, A., 2009. Caratteristiche sedimentologico- ichnologiche delle unita silicoclastiche

973 oligo-mioceniche nel transetto Pratomagno-Verghereto, Appennino Settentrionale. Annali
974 dell'Universit□a degli
975 Studi di Ferrara. Museol. Sci. Nat. 5, 23e129.
976 Monaco, P., Trecci, T., 2014. Ichnocoenoses in the macigno turbidite basin system,
977 lower miocene, trasimeno (Umbrian apennines, Italy). Ital. J. Geo. 133, 116e130.
978 http://dx.doi.org/10.3301/IJG.2013.18.
979 Monaco, P., Uchman, A., 1999. Deep-sea ichnoassemblages and ichnofabrics of the
980 Eocene Scisti varicolori beds in the Trasimeno area, western Umbria, Italy. In: Farinacci, A., Lord,
981 A.R. (Eds.), Depositional Episodes and Bioevents. Paleo- pelagos, Univ. La Sapienza, Spec. Publ.,
982 Roma, pp. 39e52.
983 Monaco, P., Milighetti, M., Checconi, A., 2009. Ichnocoenoses in the Oligocene to Miocene
984 foredeep basins (Northern Apennines, central Italy) and their relation to turbidite deposition. Acta
985 Geol. Pol. 60 (1), 53e70.
986 Monaco, P., Trecci, T., Uchman, A., 2012. Taphonomy and ichnofabric of the trace fossil
987 Avetoichnus luisae Uchman & Rattazzi, 2011 in Paleogene deep-sea fine- grained turbidites:
988 examples from Italy, Poland and Spain. Boll. Soc. Paleontol. Ital. 51 (1), 1e16.
989 Mongelli, G., Critelli, S., Perri, F., Sonnino, M., Perrone, V., 2006. Sedimentary recycling,
990 provenance and paleoweathering from chemistry and mineralogy of Mesozoic continental redbed
991 mudrocks, Peloritani Mountains, Southern Italy. Geochem. J. 40, 197e209.
992 Mongelli, G., Mameli, P., Oggiano, G., Sinisi, R., 2012. Messinian palaeoclimate and palaeo-
993 environment in the western Mediterranean realm: insights from the geochemistry of continental
994 deposits of NW Sardinia (Italy). Int. Geol. Rev. 54, 971e990.
995 http://dx.doi.org/10.1080/00206814.2011.588823.
996 Mutti, E., 1992. In: AGIP, S.p.a. (Ed.), Turbitite Sandstones. S. Donato Milanese, p. 275.
997 Muzzi Magalhaes, P., Tinterri, R., 2010. Stratigraphy and depositional setting of slurry and
998 contained (reflected) beds in the Marnoso-arenacea Fm. (Langhian Serravallian) Northern

999 Apennines, Italy. Sedimentology 57, 1685e1720. http:// dx.doi.org/10.1111/j.1365-
1000 3091.2010.01160.x.
1001 Nesbitt, H.W., Young, G.M., 1982. Early Proterozoic climates and plate motions inferred from
1002 major element chemistry of lutites. Nature 299, 715e717. http:// dx.doi.org/10.1038/299715a0.
1003 Nesbitt, H.W., Young, G.M., McLennan, S.M., Keays, R.R., 1996. Effects of chemical weathering
1004 and sorting on the petrogenesis of siliciclastic sediments, with implications for provenance studies.
1005 J. Geol. 104, 525e542.
1006 Peltola, P., Brun, C., Strom, M., Tomilia, O., 2008. High K/Rb ratios in stream waters. Exploring
1007 plant litter decay, ground water and lithology as potential controlling mechanisms. Chem. Geol.
1008 257, 92e100. http://dx.doi.org/10.1016/ j.chemgeo.2008.08.009.
1009 Pandeli, E., Ferrini, G., Lazzari, D., 1994. Lithofacies and petrography of the Macigno Fm. from the
1010 Abetone to the Monti del Chianti areas (Northern Apennines). Mem. Soc. Geol. Ital. 48, 321e329.
1011 Perri, F., 2008. Clay mineral assemblage of the TriassiceJurassic mudrocks from Western-Central
1012 mediterranean regions. Per. Mineral. 77, 23e40. http:// dx.doi.org/10.2451/2008PM0002.
1013 Perri, F., 2014. Composition, provenance and source weathering of Mesozoic sandstones from
1014 Western-Central Mediterranean Alpine Chains. J. Afr. Earth Sci.
1015 91, 32e43. http://dx.doi.org/10.1016/j.jafrearsci.2013.12.002.
1016 Perri, F., Rizzo, G., Mongelli, G., Critelli, S., Perrone, V., 2008a. Zircon compositions of lower
1017 Mesozoic redbeds of the Tethyan margins, West-Central mediterranean area. Int. Geol. Rev. 50,
1018 1022e1039. http://dx.doi.org/10.2747/0020-
1019 6814.50.11.1022.
1020 Perri, F., Cirrincione, R., Critelli, S., Mazzoleni, P., Pappalardo, A., 2008b. Clay mineral
1021 assemblages and sandstone compositions of the Mesozoic Longobucco Group, northeastern
1022 Calabria: implications for burial history and diagenetic evolution. Int. Geol. Rev. 50, 1116e1131.
1023 http://dx.doi.org/10.2747/0020-6814.50.12.1116.

1024 Perri, F., Critelli, S., Mongelli, G., Cullers, R.L., 2011a. Sedimentary evolution of the Mesozoic
1025 continental redbeds using geochemical and mineralogical tools: the case of upper triassic to
1026 lowermost Jurassic M.te di Gioiosa mudstones (Sicily, Southern Italy). Int. J. E. Sc. 100,
1027 1569e1587. http://dx.doi.org/10.1007/s00531- 010-0602-6.
1028 Perri, F., Muto, F., Belviso, C., 2011b. Links between composition and provenance of Mesozoic
1029 siliciclastic sediments from western Calabria (southern Italy). Ital. J. Geosci. 130, 318e329.
1030 http://dx.doi.org/10.3301/IJG.2011.04.
1031 Perri, F., Critelli, S., Cavalcante, F., Mongelli, G., Dominici, R., Sonnino, M., De Rosa, R., 2012a.
1032 Provenance signatures for the Miocene volcaniclastic succession of the Tufiti di Tusa Fm., southern
1033 Apennines. Italy. Geol. Mag. 149, 423e442. http:// dx.doi.org/10.1017/S001675681100094X.
1034 Perri, F., Critelli, S., Dominici, R., Muto, F., Tripodi, V., Ceramicola, S., 2012b. Prove- nance and
1035 accommodation pathways of late Quaternary sediments in the deep- water northern ionian basin,
1036 southern Italy. Sed. Geo. 280, 244e259. http:// dx.doi.org/10.1016/j.sedgeo.2012.01.007.
1037 Perri, F., Borrelli, L., Gulla□, G., Critelli, S., 2014. Chemical and minero-petrographic features of
1038 Plio-Pleistocene fine-grained sediments in Calabria, southern Italy. Ital. J. Geosci. 133, 101e115.
1039 http://dx.doi.org/10.3301/IJG.2013.17.
1040 Perri, F., Ohta, T., 2014. Paleoclimatic conditions and paleoweathering processes on Mesozoic
1041 continental redbeds from Western-Central Mediterranean Alpine Chains. Palaeogeogr.
1042 Palaeoclimatol. Palaeoecol. 395, 144e157. http:// dx.doi.org/10.1016/j.palaeo.2013.12.029.
1043 Perri, F., Dominici, R., Critelli, S., 2015. Stratigraphy, composition and provenance of argillaceous
1044 marls from the Calcare di Base Fm., Rossano Basin (northeastern Calabria). Geol. Mag. 152,
1045 193e209. http://dx.doi.org/10.1017/ S0016756814000089.
1046 Perrone, V., Perrotta, S., Marsaglia, K., Di Staso, A., Tiberi, V., 2013. The Oligocene ophiolite-
1047 derived breccias and sandstones of the Val Marecchia Nappe: insights for paleogeography and
1048 evolution of Northern Apennines (Italy). Palaeogeo. Palaeoclim. Palaeoecol. 394, 128e143.

1049 Piccioni, R., Monaco, P., 1999. Caratteri sedimentologici, ichnologici e micro- paleontologici delle
1050 unita eoceniche degli scisti varicolori nella sezione di M. Solare. Boll. Serv. Geol. D'it. 143e188.
1051 CXV.
1052 Plesi, G., Luchetti, L., Boscherin, A., Botti, F., Brozzetti, F., Bucefalo Palliani, R., Daniele, G.,
1053 Motti, A., Nocchi, M., Rettori, R., 2002. The Tuscan successions of the high Tiber Valley (Foglio
1054 289-Citta di Castello): biostratigraphic, petrographic and structural features, regional correlations.
1055 Boll. Soc. Geol. It. 121 (1), 425e436.
1056 Potter, P.E., 1978. Petrology and chemistry of modern big river sands. J. Geol. 86, 423e449.
1057 Ricci Lucchi, F., 1986. The Oligocene to recent foreland basins of the northern Apennines. Int.
1058 Assoc. Sedimentol. Spec. Publ. 8, 105e139.
1059 Ricci Lucchi, F., 1990. Turbidites in foreland and on-thrust basins of the northern Apennines.
1060 Palaeogeogr. Palaeoclimatol. Palaeoecol. 77, 51e66. http:// dx.doi.org/10.1016/0031-
1061 0182(90)90098-R.
1062 Ricci Lucchi, F., Valmori, E., 1980. Basin-wide turbidites in a Miocene, oversupplied deep-sea
1063 plain: a geometrical analysis. Sedimentology 27, 241e270. http:// dx.doi.org/10.1111/j.1365-
1064 3091.1980.tb01177.x.
1065 Roy, P.D., Caballero, M., Lozano, R., Smytatz-Kloss, W., 2008. Geochemistry of late quaternary
1066 sediments from Tecomuco lake, central Mexico: implication to chemical weathering and
1067 provenance. Chem. Erde 68, 383e393. http:// dx.doi.org/10.1016/j.chemer.2008.04.001.
1068 Sames, C.W., 1966. Morphometric data of some recent pebble associations and their applications to
1069 ancient deposits. J. Sed. Petr 36, 126e142.
1070 Schneider, R.R., Price, B., Muller, P.J., Kroon, D., Alexander, I., 1997. Monsoon-related variations
1071 in Zaire (Congo) sediment load and influence of fluvial silicate supply on marine productivity in the
1072 east equatorial Atlantic during the last 200,000 years. Paleoceanography 12, 463e481.
1073 http://dx.doi.org/10.1029/96PA03640.

1074 Shanmugan, G., 2002. Ten turbidite myths. Earth Sci. Rev. 58, 311e341. http://
1075 dx.doi.org/10.1016/S0012-8252(02)00065-X.
1076 Suttner, L.J., 1974. Sedimentary petrographic province: an evaluation. Soc. Econ. Paleontol. Miner.
1077 Spec. Publ. 21, 75e84.
1078 Talling, P.J., Amy, L.A., Wynn, R.B., Peakall, J., Robinson, M., 2004. Beds comprising debrite
1079 sandwiched within co-genetic turbidite: origin and widespread occur- rence in distal depositional
1080 environments. Sedimentology 51, 163e194. http:// dx.doi.org/10.1111/j.1365-3091.2004.00617.x.
1081 Taylor, S.R., McLennan, S.M., 1985. The Continental Crust: its Composition and Evolution.
1082 Blackwell, Oxford.
1083 Tinterri, R., Muzzi Magalhaes, P., 2011. Synsedimentary structural control on fore- deep turbidites:
1084 an example from Miocene Marnoso-arenacea Fm., Northern Apennines. Italy. Mar. Petrol. Geol.
1085 28, 629e657. http://dx.doi.org/10.1016/ j.marpetgeo.2010.07.007.
1086 Trecci, T., Monaco, P., 2011. Le ichnocenosi delle successioni sedimentarie Eocenico- Mioceniche
1087 affioranti tra il Lago Trasimeno e l'Alpe di Poti (Appennino Settentrionale). Annali di Ferrara.
1088 Museol. Sci. Nat. 7, 1e101.
1089 Trincardi, F., Verdicchio, G., Asioli, A., 2005. Comparing Adriatic contourite deposits and other
1090 Mediterranean examples. In: F.I.S.T. (Ed.), GeoItalia 2005, Spoleto 21-
1091 23 Settembre 2005, p. 321.
1092 Valloni, R., Lazzari, D., Calzolari, M.A., 1991. Selective alteration of arkose framework
1093 in Oligo-Miocene turbidites of the Northern Apeninnes foreland: impact on sedimentary
1094 provenance analysis. In: Morton, A.C., Todd, S.P., Haughtpn, P.D.W. (Eds.), 1991, Developments
1095 in Sedimentary Provenance Studies, GSA Special Publication, No 57, pp. 125e136.
1096 http://dx.doi.org/10.1144/GSL.SP.1991.057.01.11.
1097 Van de Kamp, P.C., Leake, B.E., 1985. Petrography and geochemistry of feldspathic and mafic
1098 sediments of the northeastern Pacific margin. Trans. R. Soc. Edinb. Earth Sci. 76, 411e449.

1099 Van der Meulen, M.J., Meulenkamp, J.E., Wortel, M.J.R., 1998. Lateral shifts of Apenninic
1100 foredeep depocentres reflecting detachment of subducted litho- sphere. EPSL 154, 203e219.
1101 http://dx.doi.org/10.1016/S0012-821X(97)00166-0.
1102 Walker, R.G., 1975. Generalized facies model for resedimented conglomerates of turbidite
1103 association. Bull. Geol. Soc. Am. 86, 737e748. http://dx.doi.org/ 10.1130/0016-
1104 7606(1975)86<737:GFMFRC>2.0.CO;2.
1105 Weaver, C.E., 1989. Clays, Muds, and Shales. In: Developments in Sedimentology, 44. Elsevier,
1106 Amsterdam, ISBN 0-444-87381-3, p. 819.
1107 Wrafter, J.P., Graham, J.R., 1989. Ophiolitic detritus in the Ordovician sediments of South Mayo
1108 Ireland. J. Geol. Soc. Lond. 146, 213e215. http://dx.doi.org/10.1144/ gsjgs.146.2.0213.
1109 Wronkiewicz, D.J., Condie, K.C., 1989. Geochemistry and provenance of sediments from the
1110 Pongola Supergroup, South Africa: evidence for a 3.0 Ga old conti- nental craton. Geochem.
1111 Cosmochim. Acta 53, 1537e1549. http://dx.doi.org/ 10.1016/0016-7037(89)90236-6.
1112 Wronkiewicz, D.J., Condie, K.C., 1990. Geochemistry and mineralogy of sediments from the
1113 ventersdorp and transvaal supergroup, South Africa: cratonic evolu- tion during the early
1114 Proterozoic. Geochim. Cosmochim. Acta 54, 343e354. http://dx.doi.org/10.1016/0016-
1115 7037(89)90236-6.
1116 Zaghloul, M.N., Critelli, S., Perri, F., Mongelli, G., Perrone, V., Sonnino, M., Tucker, M., Aiello,
1117 M., Ventimiglia, C., 2010. Depositional systems, composition and geochemistry of Triassic rifted
1118 continental margin redbeds of Internal Rif Chain, Morocco. Sedimentology 57, 312e350.
1119 http://dx.doi.org/10.1111/j.1365- 3091.2009.01080.x.
1120 Zuffa, G.G., 1980. Hybrid arenites: their composition and classification. J. Sed. Petrol. 50, 21e29.
1121 http://dx.doi.org/10.1306/212F7950-2B24-11D7- 8648000102C1865D.
1122 Zuffa, G.G., 1985. Optical analyses of arenites: influence of methodology on compositional results.
1123 In: Zuffa, G.G. (Ed.), Provenance of Arenites. Dordrecht, The Netherlands, NATO Advanced Study
1124 Institute Series, Reidel, 148, pp. 165e189. http://dx.doi.org/10.1007/978-94-017-2809-6_8.

1125 Zuffa, G.G., 1987. Unravelling hinterland and offshore palaeo- geography from deep- water
1126 arenites. In: Leggett, J.K., Zuffa, G.G. (Eds.), Marine Clastic Sedimentology, Models and Case
1127 Studies. Graham and Trotman, London, pp. 39e61. http:// dx.doi.org/10.1007/978-94-009-3241-
1128 8_2.

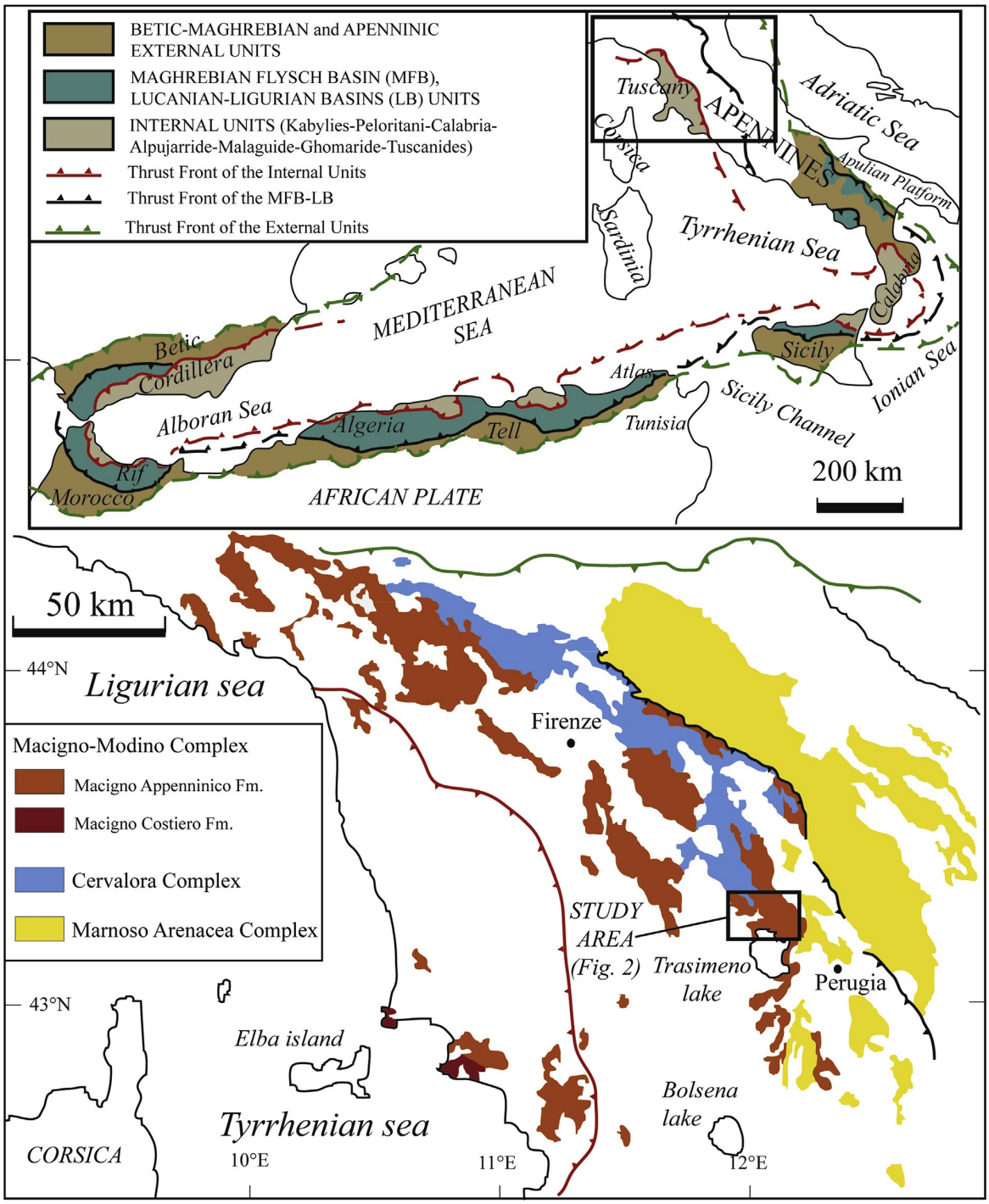

Fig. 1. Outcrop distribution of main Northern Apennines turbidite foredeep units, with indication of study area (modified after Dunkl et al., 2001).

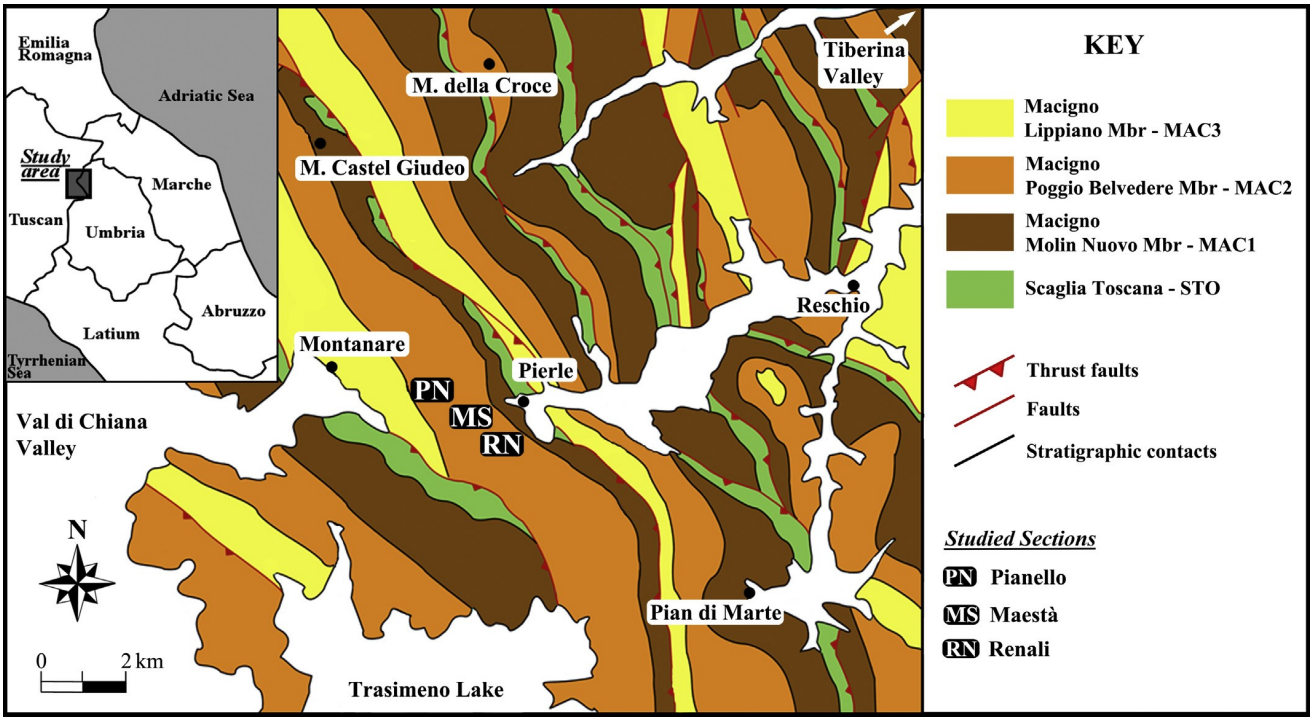

Fig. 2. Synthetic geological map of the Trasimeno Lake area showing outcrops of the Tuscan and Umbria successions and location of sections (after Monaco and Trecci, 2014).

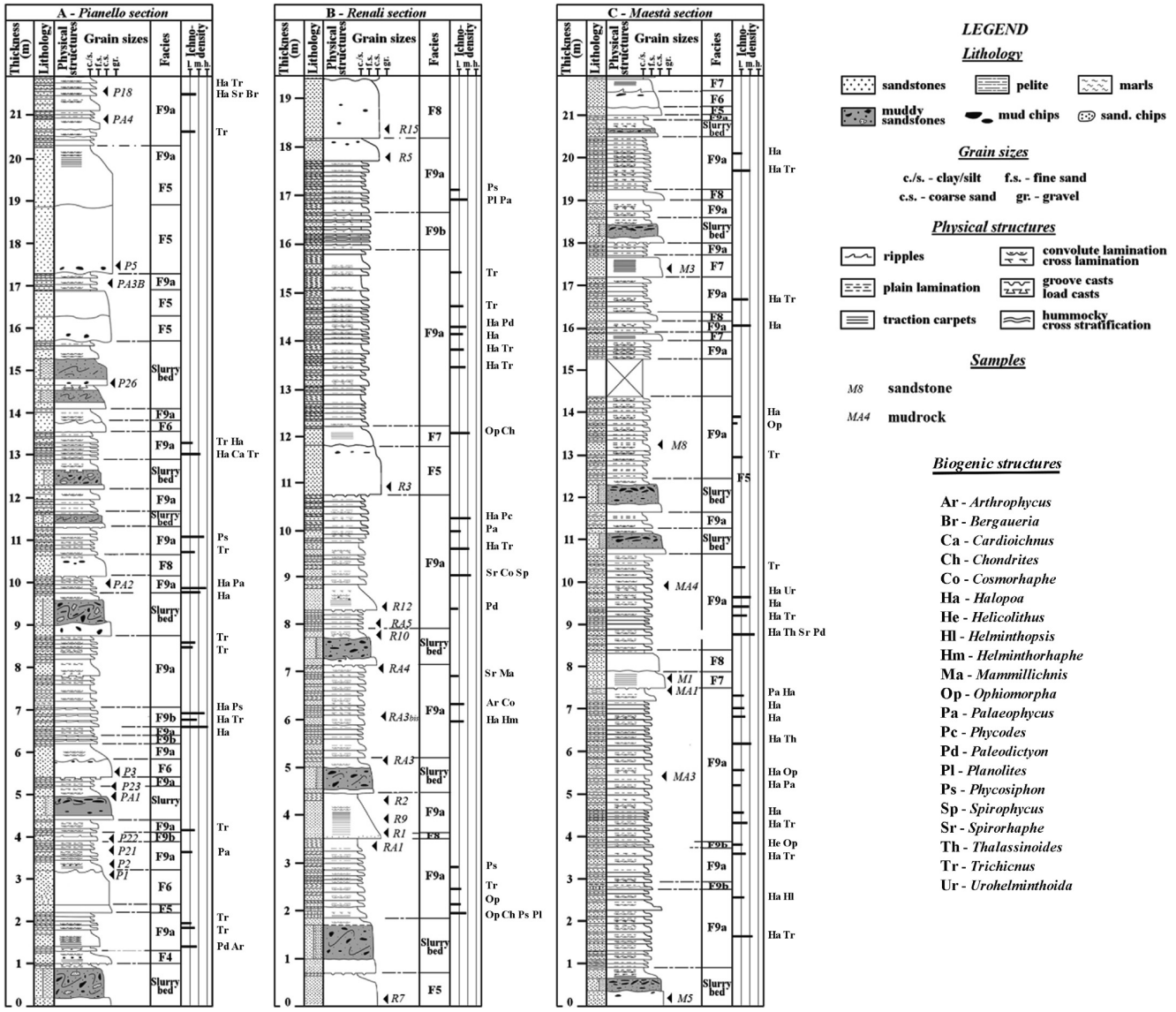

Fig. 3. Schematic synthetic stratigraphic columns of the Poggio Belvedere Member (MAC2), with the lithology and location of the studied samples. Pianello section (Lat. 43°15′08″, Long. 12°05′01″); Renali section (Lat. 43°14′41″, Long. 12°06′00″); Maestà section (Lat. 43°14′56″, Long. 12°05′41″).

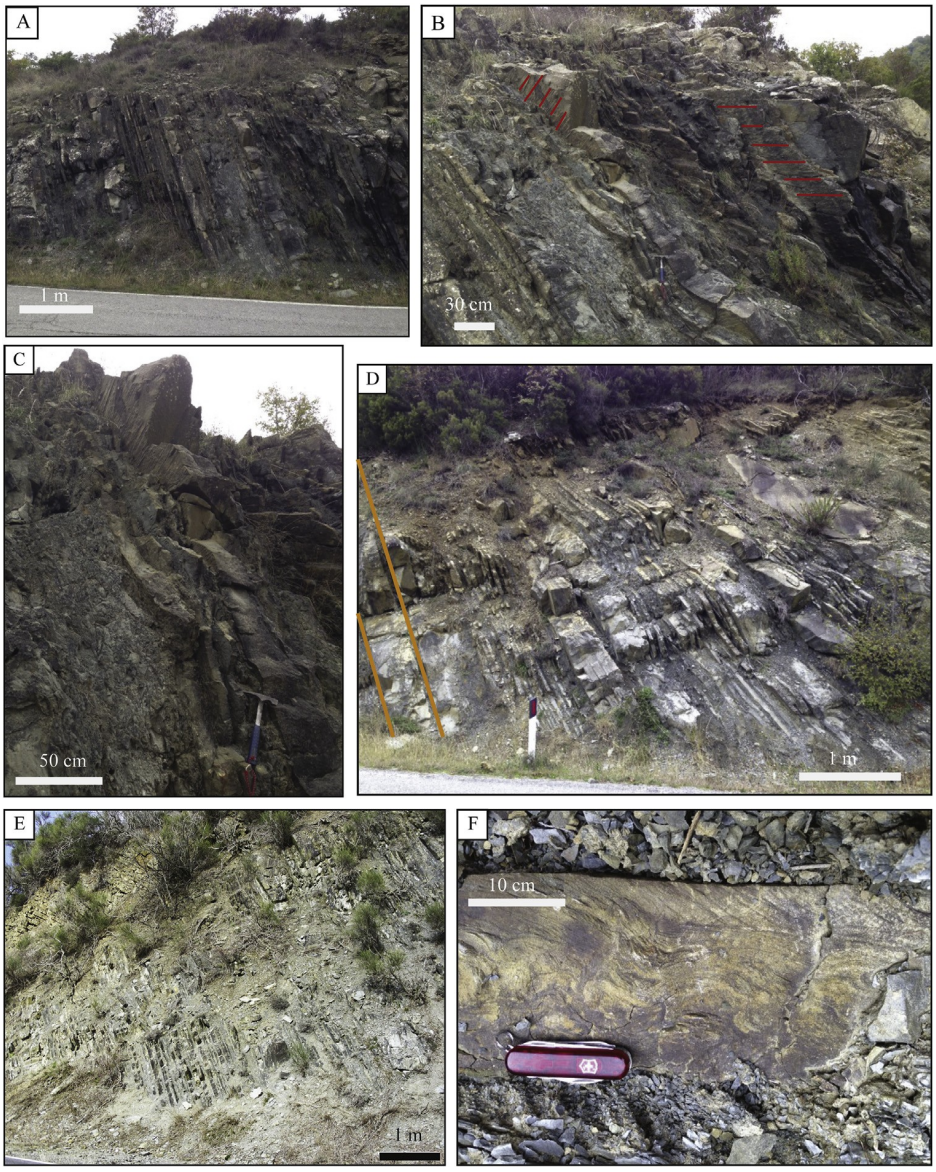

Fig. 4. Outcrops of the Poggio Belvedere Member in Trasimeno Lake area. (A) General view of the upper Pianello section deposits showing alternation between thin-bedded fine-grained turbidites (F9b facies of Mutti, 1992) and massive coarse-grained sandstones (F5eF7 facies of Mutti, 1992). (B) Detail of multidirectional lineations in sandy horizons in the uppermost portion of the Pianello Stratigraphic section (red lines indicate direction of palaeocurrents). (C) View of massive sandy horizons (F6 facies) including West-oriented flute casts in the upper Pianello Stratigraphic section. (D) View of mid-lower Renali section deposits, with presence of basal calcirudite and calcarenite levels (among yellow lines) interfingered within deep-water siliciclastic succession. (E) Alternating mudstones and fine-grained sandstones interfinged with thin massive coarse-grained sandy horizon at Maestà Stratigraphic section. (F) Detail of convolute laminations of a sandy level within fine-grained turbidite deposits (T_c of Bouma sequence) in the Maestà Stratigraphic section. (For interpretation of the references to colour in this figure legend, the reader is referred to the web version of this article.)

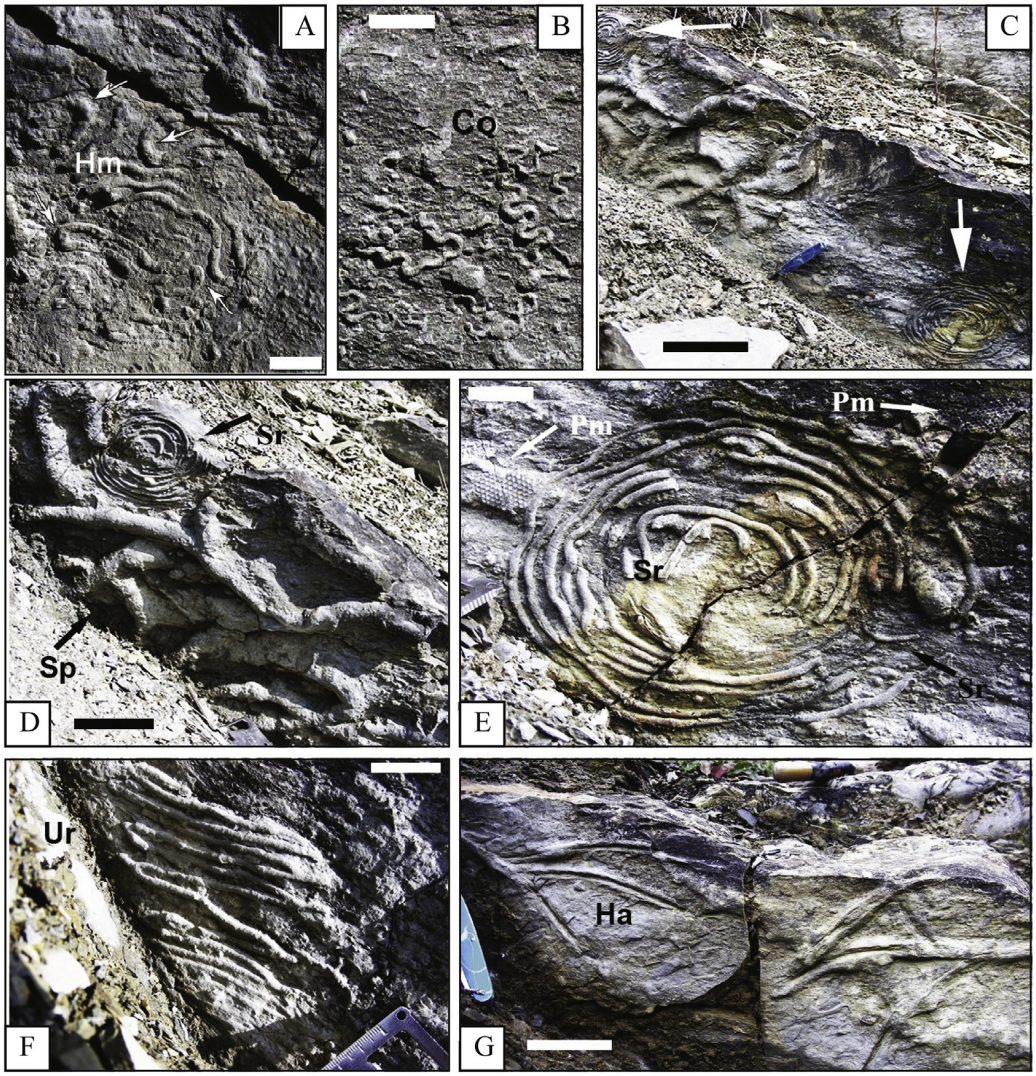

Fig. 5. Peculiar fossil traces in the studied sections. Renali Stratigraphic section (AeB): (A) The graphoglyptid *Helminthorhaphe* (Hm) at sole of turbidite with other undetermined curved specimens (arrows), bar ¼ 3 cm; (B) The graphoglyptid *Cosmorhaphe isp*. at sole of turbidite, bar ¼ 3 cm. Maestà Stratigraphic section (CeG): (C) a sole of thin turbidite with *Spirophycus* (centre) and *Spirorhaphe* (arrows), scale ¼ 10 cm; (D) a detail of *Spirophycus* (Sp) and *Spirorhaphe* (Sr), bar ¼ 10 cm; (E) a further detail on *Spirophycus bicornis* (Sp) and *Spirorhaphe* (Sr) with two *Paleodictyon minimum* specimens (Pm, arrows), bar ¼ 5; (F) the hypichnial graphoglyptid *Urohelminthoida dertonensis* at sole of turbidite, bar ¼ 5 cm; (G) Endichnial *Halopoa* (Ha, variation Fucusopsis) at sole of turbidite, bar ¼ 10 cm.

Table 1
Sandstone raw data. Categories used for sandstone samples point counts and assigned grains in recalculated plots are those of Zuffa (1985, 1987), Critelli and Le Pera (1994), and Critelli and Ingersoll (1995). R.f. = coarse grained rock fragments; NCE = noncarbonate extrabasinal grains; CI = carbonate intrabasinal grains.

		Poggio Belvedere member																		
		Pianello area									Renali area						Maestà area			
		P1	P23	P3	P5	P2	P21	P22	P18	P26	R7	R3	R12	R5	R10	R15	M1	M3	M8	M5
NCE	Quartz (single crystals)	85	39	89	54	65	90	112	85	121	87	124	89	103	116	118	105	183	142	133
	Polycrystalline quartz with tectonic fabric	6	9	17	19	14	13	12	12	5	6	10	12	7	11	7	8	6	4	4
	Polycrystalline quartz without tectonic fabric	11	8	19	10	11	12	9	16	4	4	10	5	6	13	5	3	0	4	2
	Quartz in metamorphic r.f.	3	0	4	7	1	4	2	3	0	1	3	1	7	2	1	1	0	0	2
	Quartz in plutonic r.f.	20	25	27	33	32	28	26	22	17	37	24	19	23	14	13	9	1	2	4
	Quartz in plutonic or gneissic r.f.	3	1	11	2	3	1	8	2	0	6	1	2	4	0	3	1	1	0	0
	Quartz in sandstone	0	1	0	0	0	0	0	0	0	0	0	0	0	0	0	0	0	0	0
	Calcite replacement on Quartz	7	7	15	4	20	12	17	59	22	15	28	31	17	20	27	17	6	25	1
	K-feldspar (single crystals)	33	29	17	8	32	27	11	17	30	24	10	11	22	14	21	21	3	19	17
	K-feldspar in metamorphic r.f.	0	1	2	1	0	1	7	1	0	0	0	0	0	0	0	0	0	0	1
	K-feldspar in plutonic r.f.	10	17	9	11	4	6	0	5	5	6	3	1	5	3	2	3	0	3	0
	K-feldspar in plutonic or gneissic r.f.	0	1	2	0	1	1	0	0	0	2	0	0	0	0	1	1	0	0	0
	K-feldspar in sandstone	0	0	0	0	0	0	0	0	0	0	1	0	0	0	0	0	0	0	0
	Calcite replacement on K-feldspar	2	2	3	9	3	1	4	4	10	1	0	0	0	1	3	1	0	5	0
	Plagioclase (single crystals)	59	53	36	35	34	39	32	27	51	35	43	58	35	35	45	55	37	34	65
	Plagioclase in metamorphic r.f.	1	4	0	5	0	0	1	0	0	0	0	1	1	1	0	0	0	0	0
	Plagioclase in plutonic r.f.	14	20	14	45	20	20	17	4	3	21	7	9	12	5	10	8	0	4	4
	Plagioclase in plutonic or gneissic r.f.	2	3	1	3	2	0	0	1	0	0	0	4	1	1	0	1	0	0	1
	Plagioclase in sandstone	0	1	0	0	0	0	0	0	0	0	0	0	0	0	0	0	0	0	0
	Calcite replacement on Plagioclase	16	12	5	19	20	9	9	12	12	5	3	9	1	16	7	11	0	5	0
	Micas and chlorite (single crystals)	21	16	12	25	27	24	34	35	28	34	19	23	41	29	37	50	67	49	69
	Micas and chlorite in plutonic r.f.	4	3	3	1	4	3	11	5	0	3	1	0	3	2	0	0	0	0	0
	Micas and chlorite in metamorphic r.f.	2	1	0	1	0	0	1	0	0	2	0	0	2	0	0	0	0	0	0
	Micas and chlorite in plutonic or gneissic r.f.	0	1	1	0	0	3	0	0	0	0	1	2	2	0	0	0	0	1	1
	Volcanic lithic with felsic granular texture	0	4	1	0	0	0	0	0	0	1	0	0	0	0	0	0	0	0	0
	Volcanic lithic with microlithic texture	0	0	0	0	0	0	0	0	0	2	0	0	2	1	0	0	0	0	0
	Other volcanic lithic	0	0	0	0	0	0	0	0	0	7	0	1	3	0	0	0	0	0	0
	Phyllite	5	3	6	6	4	2	0	3	0	3	3	1	2	1	0	0	0	1	0
	Fine grained schists	3	5	3	2	1	0	1	2	2	5	0	4	2	3	2	3	1	1	2
	Impure chert	1	2	2	2	0	2	0	0	1	0	2	2	0	1	0	5	2	1	0
	Sedimentary lithic	0	13	0	1	2	1	3	0	0	0	3	11	3	9	3	0	0	0	1
	Slate	3	4	1	1	1	1	1	1	1	2	4	2	1	1	0	0	0	0	1
	Chlorite/Muscovite schist	0	3	0	1	0	0	0	0	0	0	0	2	2	1	1	3	0	0	4
CE	Bioclasts	0	0	0	0	0	0	0	0	0	0	0	0	0	12	1	0	0	0	0
Mx	Siliciclastic matrix	46	30	56	4	41	54	33	1	40	24	28	31	49	79	3	28	2	12	30
	Epi matrix	1	0	2	3	2	1	3	1	0	0	0	0	0	1	4	1	3	3	0
	Pseudomatrix	0	0	0	6	17	4	1	3	0	1	1	2	2	0	1	4	6	3	7
Cm	Carbonate cement (pore-filling)	0	4	0	1	0	4	0	68	2	0	0	0	0	0	2	0	0	2	0
	Carbonate cement (patchy-calcite)	0	0	0	2	0	2	0	0	6	2	2	4	2	4	0	0	0	1	0
	Calcite replacement on undetermined grains	0	4	2	2	0	2	2	3	2	3	1	1	4	4	0	0	0	1	0
	Quartz overgrowth	0	1	0	0	0	0	0	0	0	0	0	0	0	0	0	0	0	0	0
TOT		358	327	360	323	361	367	357	392	362	339	332	338	364	400	317	339	318	322	349

Table 2
Recalculated modal point count data.

Section	Facies	Sample	%			%			%			%			%			%			%			Index			
			Qm	F	Lt	Qt	F	L	Qm	K	P	Qp	Lvm	Lsm	Lm	Lv	Ls	Rg	Rv	Rm	Rg	Rs	Rm	Lv/L	P/F	Q/F	F/L
Maestà area	slurried div.	M5	58	36	6	60	37	3	61	8	31	43	0	57	92	0	8	42	0	58	40	4	56	0	0.79	1.59	6.29
	basin plain	M8	68	28	4	71	28	1	70	12	18	82	0	18	86	0	14	63	0	37	59	6	35	0	0.61	2.41	6.36
	outer lobe	M3	79	17	4	83	16	1	83	1	16	89	0	11	78	0	22	22	0	78	18	18	64	0	0.92	4.77	4.44
	outer lobe	M1	52	39	9	58	39	3	57	11	32	73	0	27	74	0	26	61	0	39	53	12	35	0	0.74	1.32	4.59
		outer lobe	66	28	6	71	27	2	70	6	24	81	0	19	76	0	24	42	0	58	36	15	49	0	0.83	3.045	4.52
		X	***64***	***30***	***6***	***68***	***30***	***2***	***68***	***8***	***24***	***72***	***0***	***28***	***82***	***0***	***17.5***	***47***	***0***	***53***	***42.5***	***10***	***47.5***	***0***	***0.76***	***2.52***	***5.42***
		s.d.	***12***	***9.83***	***2.36***	***12***	***10***	***1.15***	***12***	***5***	***8.42***	***20***	***0***	***20***	***8.06***	***0***	***8.06***	***19***	***0***	***19***	***18***	***6.32***	***15***	***0***	***0.13***	***1.57***	***1.05***
Renali area	slurried div.	R15	65	27	8	65	33	2	64	11	25	67	0	33	71	0	29	72	0	28	67	7	26	0	0.7	1.82	4.94
	slurried div.	R10	54	27	19	66	28	6	67	8	25	61	2	37	42	3	55	54	2	44	46	18	36	0.04	0.76	2	1.81
		slur.div.	59.5	27	13	65	31	4	66	9	25	64	1	35	56.5	1	42	63	1	36	57	12	31	0.02	0.73	1.91	3.375
	basin plain	R5	59	30	11	64	30	6	67	12	21	46	18	36	63	23	14	63	6	31	64	4	32	0.23	0.65	2	2.75
	basin plain	R12	52	34	14	58	34	8	60	5	35	47	3	50	60	3	37	66	1	33	56	16	28	0.03	0.87	1.53	2.32
		basin	56	32	12	61	32	7	64	8	28	46	11	43	61	13	26	64	4	32	60	10	30	0.13	0.76	1.765	2.535
	outer lobe	R3	67	25	8	72	24	4	73	6	21	69	0	31	77	0	23	65	0	35	59	9	32	0	0.79	2.69	2.09
	outer lobe	R7	54	35	11	58	35	7	61	14	25	33	34	33	62	38	0	72	10	18	80	0	20	0.38	0.65	1.55	3.13
		outer lobe	61	30	9	65	30	5	67	10	23	51	17	32	69	19	11.5	68	5	27	70	4	26	0.19	0.72	2.12	2.61
		X	***58.5***	***30***	***12***	***64***	***31***	***5***	***65***	***10***	***25***	***54***	***9***	***37***	***62.5***	***11***	***26***	***65***	***3***	***31.5***	***62***	***9***	***29***	***0.11***	***0.74***	***1.93***	***2.84***
		s.d.	***6.28***	***4.08***	***4.17***	***5.31***	***4.18***	***2.17***	***4.76***	***3.56***	***5.13***	***14***	***14***	***6.89***	***12***	***16***	***19***	***6.68***	***4***	***8.55***	***11***	***6.93***	***5.62***	***0.16***	***0.09***	***0.43***	***1.13***
Pianello area	slurried div.	P26	56	39	5	60	39	1	59	17	24	77	0	23	89	0	11	76	0	24	73	3	24	0	0.59	1.44	8.54
	fringe-basin	P18	62	26	12	72	26	2	71	11	18	82	0	18	100	0	0	64	0	36	64	0	36	0	0.62	2.4	2.09
	fringe-basin	P22	62	30	8	68	30	2	67	9	24	81	0	19	78	0	22	71	0	29	69	3	28	0	0.73	2.03	3.11
	fringe-basin	P21	50	39	11	60	39	1	57	15	28	87	0	13	84	0	16	75	0	25	72	3	25	0	0.65	1.29	3.35
	fringe-basin	P2	45	43	12	54	43	3	51	17	32	76	0	24	91	0	9	90	0	10	88	3	9	0	0.65	1.04	3.51
		fringe-basin	55	34	10.75	63	35	2	62	13	25	81	0	19	88.25	0	11.75	75	0	25	73	2	25	0	0.6625	1.69	3.015
	outer lobe	P5	36	49	15	47	49	4	43	12	45	74	0	26	91	0	9	69	0	31	67	2	31	0	0.78	0.73	3.48
	outer lobe	P3	52	31	17	65	31	4	62	14	24	78	2	20	90	3	7	66	1	33	66	2	32	0.09	0.63	1.64	1.82
	outer lobe	P23	27	54	19	35	54	11	34	23	43	37	8	55	56	9	35	68	4	28	61	14	25	0.09	0.65	0.51	2.8
	outer lobe	P1	42	48	10	48	48	4	46	18	36	62	0	38	94	0	6	70	0	30	69	1	30	0	0.67	0.86	4.72
		outer lobe	39	46	15.25	49	45	6	46	17	37	63	2	35	82.75	3	34	68	1	31	66	5	29	0.045	0.6825	0.935	3.205
		X	***48***	***40***	***12***	***57***	***40***	***3***	***54***	***15***	***30***	***73***	***1***	***26***	***86***	***1***	***13***	***72***	***1***	***27***	***70***	***3***	***27***	***0.02***	***0.66***	***1.327***	***3.713***
		s.d.	***12***	***9.55***	***4.37***	***12***	***9.55***	***3***	***12***	***4.23***	***9.28***	***15***	***2.67***	***13***	***13***	***3***	***10***	***7.74***	***1.33***	***7.48***	***7.75***	***4.1***	***7.48***	***0.04***	***0.058***	***0.621***	***2***

Note: X = mean, s.d = standard deviation. Qm = monocrystalline quartz, Qp = polycrystalline quartz, F = feldspars (K+P), K = K-feldspar, P = plagioclase; Lt = lithic grains; Lm = metamorphic, Lv = volcanic, and Ls = sedimentary lithic grains; Lvm = volcanic and metavolcanic, Lsm = sedimentary and metasedimentary lithic grains; Rg = phaneritic plutonic rock fragments; Rm = coarse and fine grained metamorphic rock fragments; Rv = coarse and fine grained volcanic rock fragments; Rs = coarse and fine grained sedimentary rock fragments.

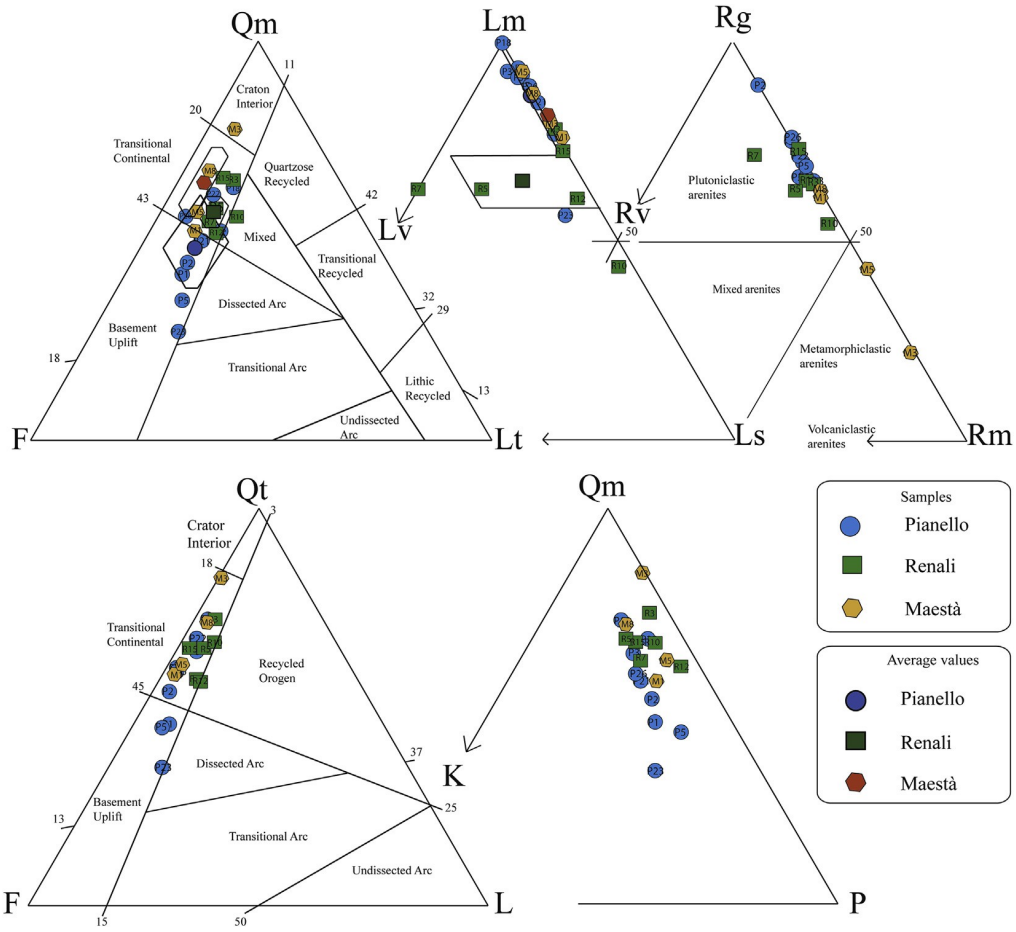

Fig. 6. QmeFeLt, LmeLveLs, RgeRseRm QteFeL and QmeKeP triangular plots (from Dickinson, 1970; Ingersoll and Suczek, 1979; Critelli and Le Pera, 1994; Folk, 1968; Graham et al., 1976) for Poggio Belvedere sandstones of the Macigno Fm. Qm (monocrystalline quartz), F (feldspars) and Lt (total lithic fragments); Lm (metamorphic), Lv (volcanic) and Ls (sedimentary) lithic fragments; Rg (plutonic rock fragments), Rv (volcanic rock fragments) and Rm (metamorphic rock fragments); Qt (quartz grains), F (feldspars) and L (aphanitic lithic fragments); Qm (monocrystalline quartz), K (K-feldspar) and P (plagioclase).

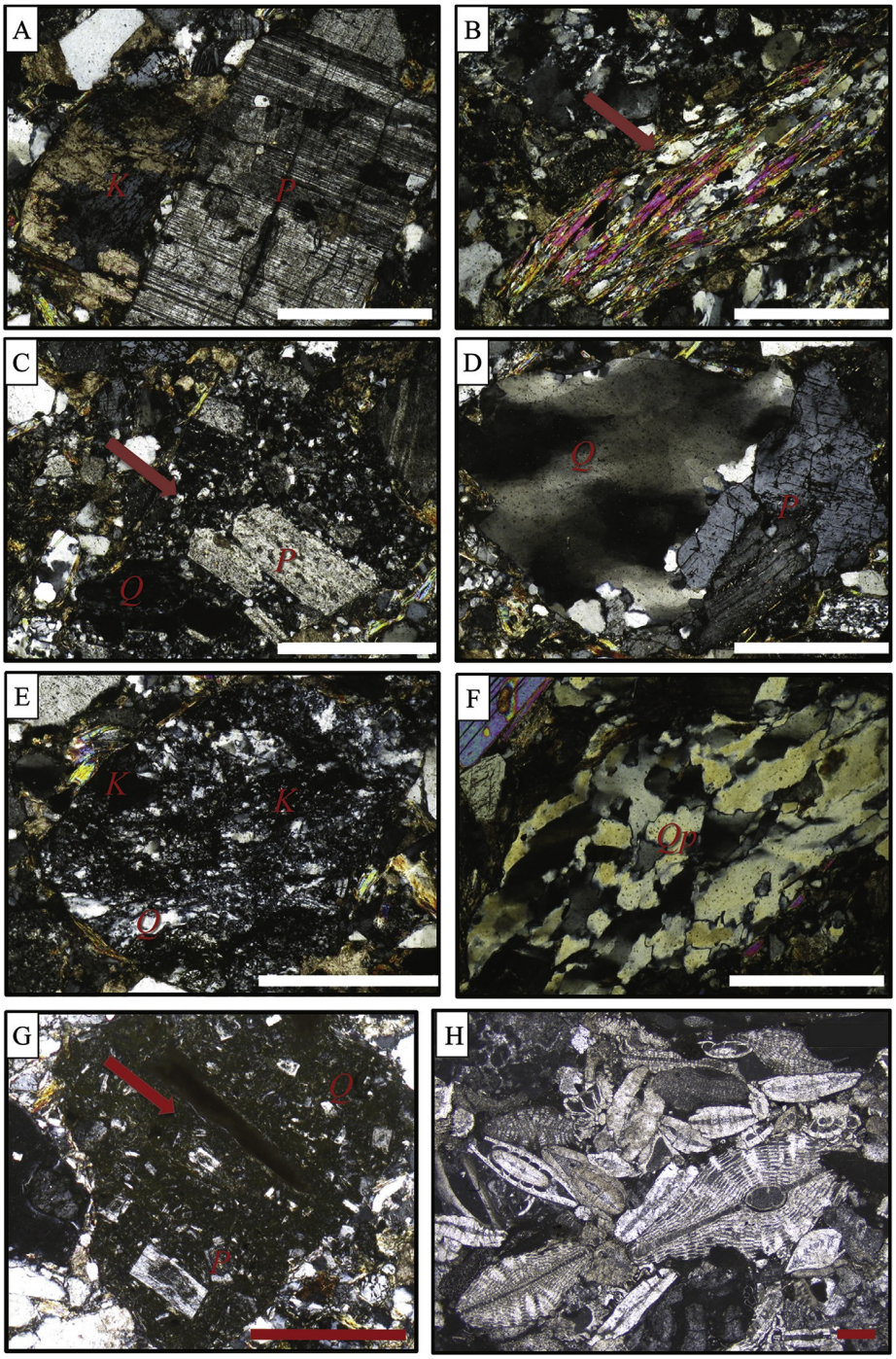

Fig. 7. Peculiar granular components in sandstones (crossed nicols view), bar ¼ 500 mm. (A) Plagioclase displaying typical albite polysynthetic twinning (*P*) and K-feldspar grains (*K*) locally replaced by calcite cement. (B) Fine-grained schist (*red arrow*) with internal muscovite and quartz grains. (C) Volcanic rock fragment with felsic granular fabric (*red arrow*) including internal plagioclase (*P*) and quartz (*Q*) phenocrysts. (D) Plutonic rock fragment with quartz (*Q*) and plagioclase crystals (*P*). (E) Metamorphic rock fragment with isoriented strips of quartz (*Q*) and K-feldspar (*K*). (F) Polycristalline quartz grain with tectonic fabric (*Qp*). (G) Volcanic rock fragment with microlithic fabric (*red arrow*) containing phenocrysts of plagioclase (*P*) and quartz (Q) in a fine-grained groundmass rich in K. (H) Packstone with macroforaminifers (lepidocyclinids and nummulitids). (For interpretation of the references to colour in this figure legend, the reader is referred to the web version of this article.)

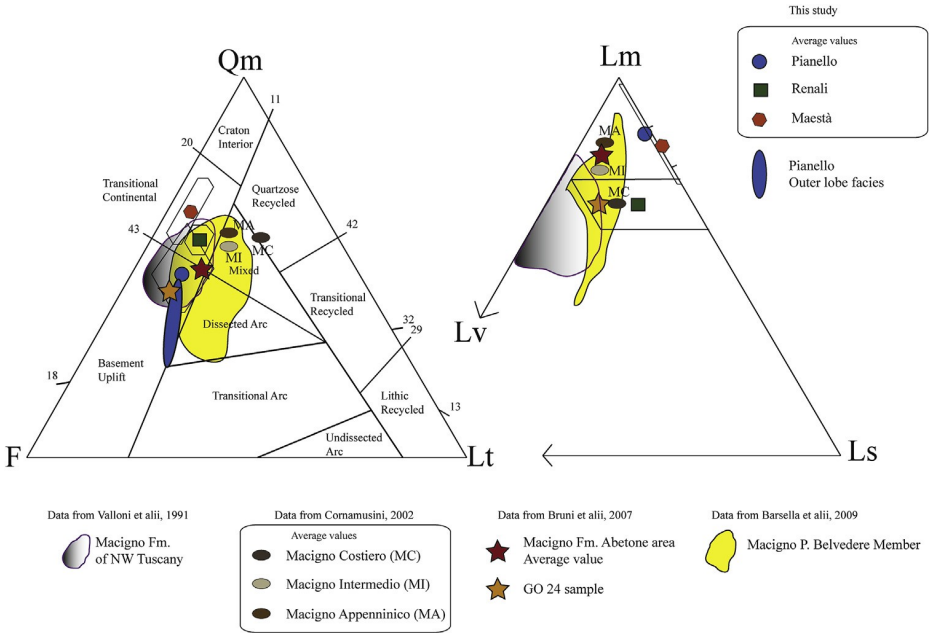

Fig. 8. Comparisons of studied data with previous works using QmeFeLt and LmeLveLs diagram plots (from Dickinson, 1970; Ingersoll and Suczek, 1979). Qm (monocrystalline quartz), F (feldspars) and Lt (total lithic fragments); Lm (metamorphic), Lv (volcanic) and Ls (sedimentary) lithic fragments.

Table 3

Average petrological parameters and ratios of Poggio Belvedere sandstones compared with Macigno sandstones and Calabrian arc sands (after Ibbeken and Schleyer, 1991; Perri et al., 2012b); standard deviation in brackets.

Clastic system	Petrological parameters and ratios										
	Qm	F	Lt	Lm	Lv	Ls	Lv%	Iv%	Q/F	F/L	P/F
Poggio Belvedere sandstones (this study)											
Maestà area	64 (12)	30 (10)	6 (2)	82 (8)	0	18 (8)	0	0	2.52	5.42	0.76
Renali area	59 (6)	30 (4)	12 (4)	63 (12)	11 (16)	26 (19)	14	11.25	1.93	2.84	0.74
Pianello area	48 (12)	40 (10)	12 (4)	86 (13)	1 (3)	13 (10)	4-2,5	2	1.33	3.71	0.66
Macigno sandstones e *northern Tuscany* (Di Giulio, 1999)											
Upper Macigno	54 (4)	29 (4)	17 (3)	84 (5)	11 (3)	5 (2)	…	…	1.9	1.8	…
Lower Macigno	55 (5)	26 (3)	19 (5)	70 (7)	21 (6)	9 (5)	…	…	2.2	1.5	…
Macigno sandstones e *Tuscany* (Cornamusini, 2002)											
Macigno Costiero petrofacies	57 (4)	19 (4)	24 (7)	66 (5)	19 (8)	15 (8)	≥13 ≥ 13	19	3	0.79	0.3
Macigno Intermedio petrofacies	55 (4)	27 (2)	18 (5)	75 (7)	19 (7)	6 (5)	≥13 ≥ 13	19	2.03	1.5	0.4
Macigno Appenninico petrofacies	59 (6)	25 (4)	16 (4)	82 (8)	11 (5)	7 (5)	<13	11.5	2.36	1.56	0.45
Macigno sandstones e *Northern Umbria* (Plesi et al., 2002)											
Poggio Belvedere member	40e55	20e50	10 e25	…	…	…	…	…	0.8e2.75	0.8e5	0.62
Macigno sandstones e *NW Tuscany* (Bruni et al., 2007)											
Upper Macigno	50 (6)	34 (8)	16 (4)	74 (9)	15 (7)	11 (8)	…	…	1.47	2.125	…
Lower Macigno	52 (3)	32 (4)	16 (2)	79 (8)	13 (6)	8 (5)	…	…	1.625	2	…
Macigno sandstones e *E Tuscany/W Umbria* (Barsella et al., 2009)											
Molin Nuovo member	49e74	28e42	9e26	42e59	30e38	6e20			1.2e2.6	1e4.7	…
Poggio Belvedere member	36e61	14e24	10e25	52e89	6e33	4e15	…	…	1.5e4.3	0.96e1.4	…
Modern Calabria Arc sands											
Granite sourced sands*	46	33	21	…	…	…	…	…	1.3	3.3	…
Metamorphic sourced sands*	55	24	21	…	…	…	…	…	2.4	1.4	…
Average*	51	28	21	88	0	12	0	0	1.82	1.33	…
Neto-Lipuda petrofacies**	36	46	18	86	0	14	0	0	0.78	2.55	0.7

Note: *Data reported after Ibbeken and Schleyer, 1991; ** Data reported after Perri et al., 2012b.

Table 4
Mineralogical composition of the bulk rock (weight percent).

Section	Sample	Exp (I/S)	Exp (Chl/S)	Illite- micas	Kao	Chl	S Phy	Qtz	K-feld	Pl	Cal	Dol
Maestà area	MA4	1	1	32	tr	22	56	22	1	12	7	0
	MA1	1	1	29	tr	25	56	22	1	15	5	0
	MA3	3	2	37	1	19	62	26	1	9	2	0
Renali area	RA5	3	2	53	1	10	69	24	1	4	1	0
	RA4	2	2	32	tr	12	48	22	2	19	9	0
	RA3bis	1	1	32	tr	15	49	23	1	16	10	0
	RA3	2	1	32	tr	14	49	23	1	15	11	0
	RA1	1	1	35	tr	20	57	22	1	13	7	0
Pianello area	PA4	1	1	35	2	14	53	20	2	13	11	0
	PA3A	1	1	33	2	13	50	25	2	17	5	0
	PA2	2	1	48	1	13	65	24	2	7	2	tr
	PA1	1	2	34	tr	16	53	24	2	15	5	tr

Table 5
Major, trace element and ratios distribution of mudstone samples.

Sample	Pianello area				Renali area					Maestà area		
	PA1	PA2	PA3A	PA4	RA1	RA3	RA3bis	RA4	RA5	MA1	MA3	MA4
Oxides (wt%)												
SiO_2	53.29	53.17	53.05	48.04	50.56	49.66	49.76	50.64	52.57	49.44	54.30	49.65
TiO_2	0.80	0.89	0.82	0.80	0.82	0.78	0.81	0.79	0.99	0.86	0.85	0.84
Al_2O_3	15.81	17.82	15.54	14.82	15.55	14.26	14.74	14.65	18.61	15.37	17.12	15.28
Fe_2O_3	7.03	5.86	7.06	7.38	7.88	7.53	7.55	7.38	5.74	8.59	7.11	7.90
MnO	0.07	0.08	0.08	0.08	0.08	0.08	0.08	0.09	0.04	0.08	0.06	0.09
MgO	6.75	5.73	6.28	6.58	6.42	5.81	6.17	6.25	6.37	9.69	6.58	8.11
CaO	3.33	1.65	3.81	7.03	4.71	6.86	6.16	5.97	1.34	3.33	1.72	4.67
Na_2O	1.17	0.51	1.28	0.63	0.89	1.16	1.03	1.08	0.25	0.80	1.01	0.99
K_2O	3.59	4.43	3.39	3.54	3.44	2.99	3.22	3.20	5.11	2.95	4.08	3.10
P_2O_5	0.11	0.08	0.12	0.08	0.08	0.11	0.10	0.11	0.05	0.08	0.10	0.09
LOI	7.33	9.35	7.70	11.00	9.31	9.93	9.91	9.41	8.57	8.71	6.66	9.04
Tot	99.28	99.57	99.12	99.98	99.74	99.17	99.51	99.56	99.64	99.90	99.58	99.76
Trace elements (ppm)												
V	154.00	178.00	164.00	175.00	164.00	141.00	160.00	152.00	180.00	176.00	164.00	168.00
Cu	36.88	33.23	42.14	34.08	45.21	17.76	50.39	59.46	35.80	48.16	32.80	45.19
Co	20.62	22.70	21.22	29.99	31.88	20.82	22.97	18.61	20.56	32.31	17.62	34.51
Cr	132.00	237.00	158.00	196.00	247.00	107.00	173.00	177.00	243.00	592.00	188.00	393.00
Ni	90.47	137.89	101.60	164.48	168.86	85.79	133.06	136.12	152.40	363.56	108.28	266.88
Zn	119.52	111.38	117.22	134.23	145.62	113.41	137.94	139.97	101.54	129.40	131.52	130.47
Sr	141.00	103.00	150.00	249.00	190.00	228.00	247.00	224.00	96.00	129.00	101.00	185.00
Ba	479.00	346.00	471.00	417.00	463.00	439.00	434.00	435.00	300.00	393.00	444.00	438.00
Rb	193.00	254.00	179.00	197.00	187.00	146.00	170.00	164.00	304.00	156.00	221.00	159.00
Y	32.00	31.00	28.00	31.00	28.00	21.00	34.00	35.00	40.00	29.00	30.00	30.00
Zr	177.00	183.00	168.00	128.00	138.00	147.00	152.00	157.00	197.00	156.00	172.00	155.00
Nb	17.00	20.00	18.00	18.00	17.00	16.00	17.00	15.00	23.00	16.00	19.00	16.00
La	43.00	60.00	39.00	36.00	29.00	16.00	35.00	39.00	69.00	40.00	57.00	43.00
Ce	84.00	134.00	69.00	91.00	75.00	64.00	96.00	97.00	144.00	86.00	109.00	84.00
Ratios												
CIA	66.48	68.05	66.89	68.44	64.80	68.72	67.10	67.62	66.47	70.43	68.54	70.20
CIA'	68.54	69.95	68.65	69.79	70.08	69.35	69.47	69.21	69.04	72.80	68.68	71.03
ICV	1.43	1.07	1.46	1.75	1.55	1.76	1.69	1.68	1.06	1.71	1.25	1.68
LaÞCe/Cr	0.96	0.82	0.68	0.65	0.42	0.75	0.76	0.77	0.88	0.21	0.88	0.32
LaÞCe/Co	6.16	8.55	5.09	4.23	3.26	3.84	5.70	7.31	10.36	3.90	9.42	3.68
LaÞCe/Ni	1.40	1.41	1.06	0.77	0.62	0.93	0.98	1.00	1.40	0.35	1.53	0.48
Al/K	4.40	4.02	4.59	4.19	4.52	4.77	4.58	4.58	3.64	5.21	4.19	4.93
Rb/K	0.005	0.006	0.005	0.006	0.005	0.005	0.005	0.005	0.006	0.005	0.005	0.005
Cr/V	0.86	1.33	0.96	1.12	1.51	0.76	1.08	1.16	1.35	3.36	1.15	2.34
Y/Ni	0.35	0.22	0.28	0.19	0.17	0.24	0.26	0.26	0.26	0.08	0.28	0.11

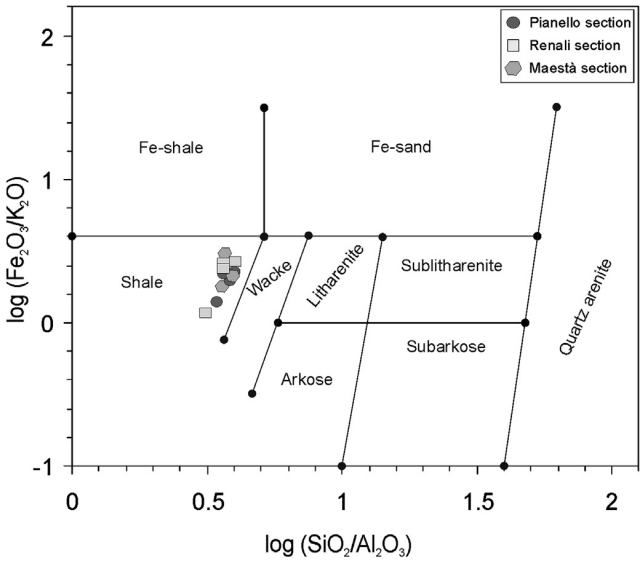

Fig. 9. Classification diagram for the studied mudstone samples (Herron, 1988).

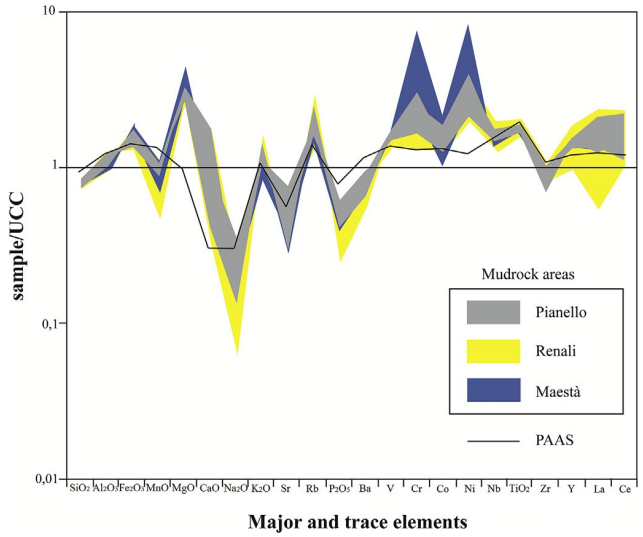

Fig. 10. Normalization of major and trace elements to the upper continental crust (UCC; McLennan et al., 2006). The plot of the Post-Archean Australian Shales (PAAS; Taylor and McLennan, 1985) is shown for comparison.

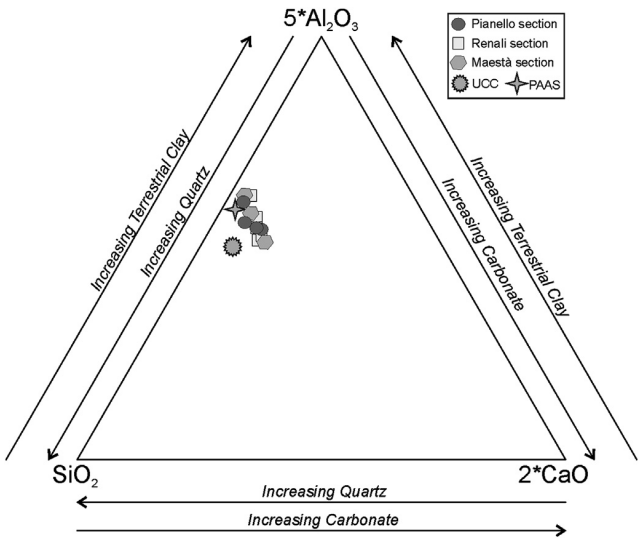

Fig. 11. Ternary plot showing the relative proportions of SiO_2 (representing quartz), Al_2O_3 (representing mica/clay minerals), and CaO (representing carbonate) for the studied mudstone samples.

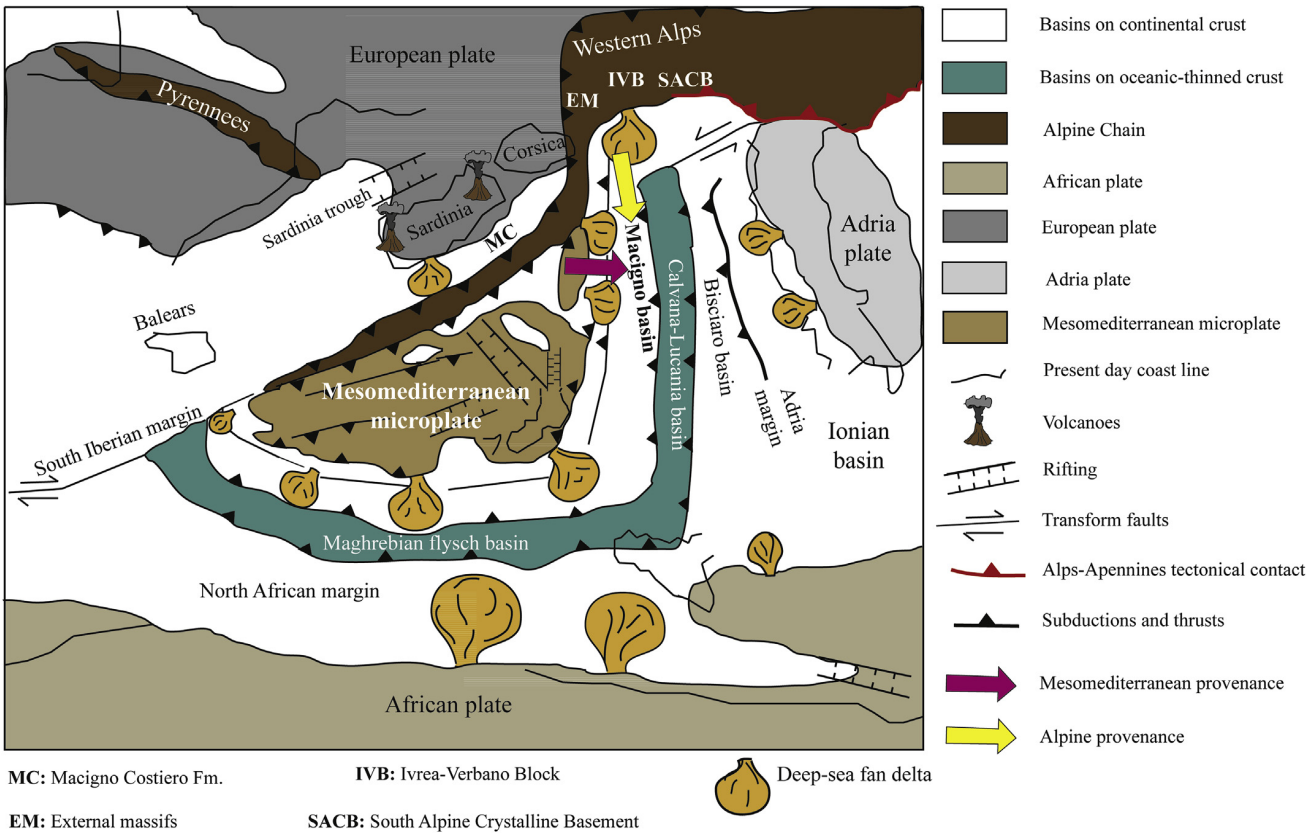

Fig. 12. Palaeogeographic and geodynamic model of the central-western Mediterranean area showing the possible source areas for Macigno foredeep system (modified after Guerrera et al., 2015).

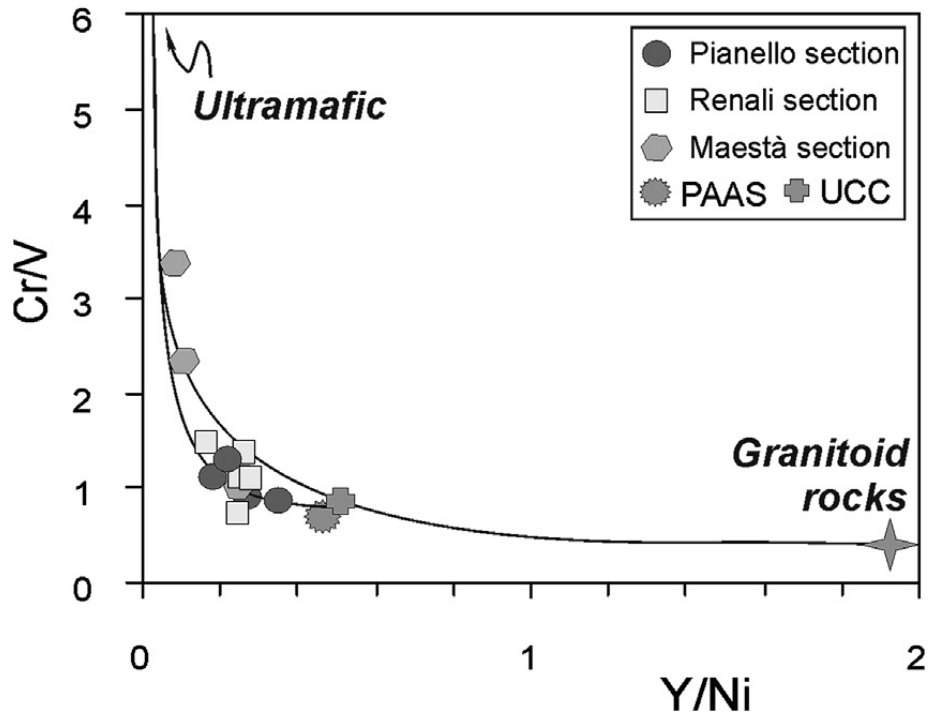

Fig. 13. Provenance diagram based on the Cr/V vs. Y/Ni relationships (after Hiscott, 1984). Curve model mixing between felsic and ultramafic end-members.

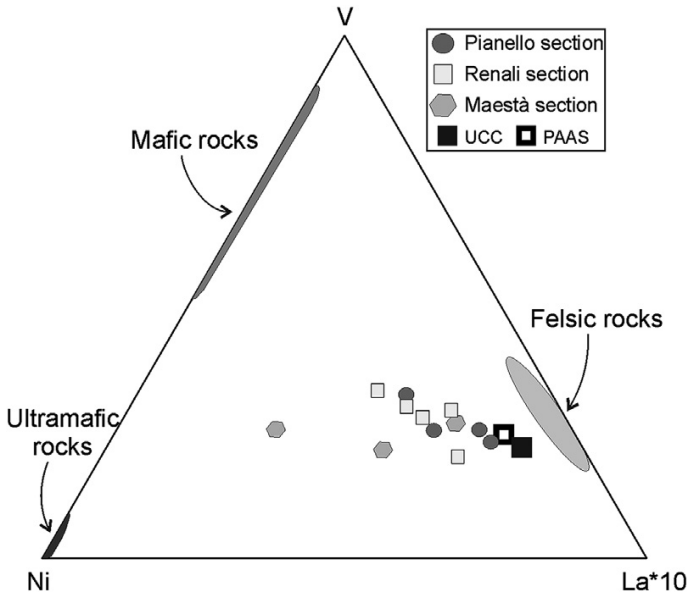

Fig. 14. V–Ni–La*10 ternary diagram, showing fields representative of felsic, mafic and ultramafic rocks plot separately (e.g., Bracciali et al., 2007; Perri et al., 2011b).

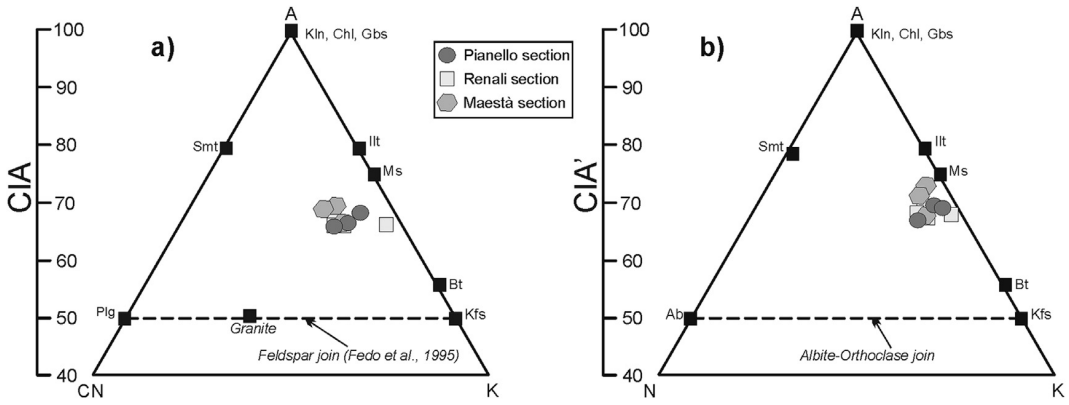

Fig. 15. Ternary (A) A–CN–K (Nesbitt and Young, 1982) and (B) A–C–N (Perri et al., 2014, 2015) plots. Key: A, Al_2O_3; C, CaO; N, Na_2O; K, K_2O; Gr, granite; Ms, muscovite; Ilt, illite; Kln, kaolinite; Chl, chlorite; Gbs, gibbsite; Smt, smectite; Plg, plagioclase; Kfs, K-feldspar; Bt, biotite; Ab, albite.

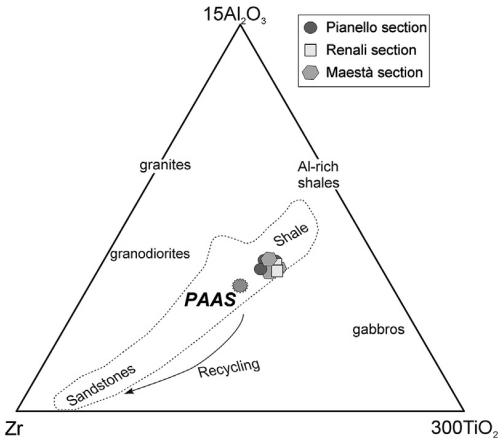

Fig. 16. Ternary $15^*Al_2O_3$–300^*TiO_2–Zr plot after García et al. (1994) for the studied mudstone samples.